IEEE Access
Multidisciplinary | Rapid Review | Open Access Journal

Received 19 July 2022, accepted 18 August 2022, date of publication 21 September 2022, date of current version 28 September 2022.

Digital Object Identifier 10.1109/ACCESS.2022.3208235

RESEARCH ARTICLE

Protocol Solutions for IEEE 802.11bd by Enhancing IEEE 802.11ad to Address Common Technical Challenges Associated With mmWave-Based V2X

RAFID I. ABD, (Member, IEEE), AND KWANG SOON KIM, (Senior Member, IEEE)
School of Electrical and Electronic Engineering, Yonsei University, Seoul 03722, South Korea

Corresponding author: Kwang Soon Kim (ks.kim@yonsei.ac.kr)

This work was supported in part by the National Research Foundation of Korea (NRF) through the Korea Government (MSIT) under Grant 2019R1A2C2007982; and in part by the Institute for Information and Communications Technology Promotion (IITP) through the Korea Government, Ministry of Science and Information and Communications Technology (ICT) Industry (MSIT), under Grant 2021-0-02208.

ABSTRACT A multi-gigabit (WiGig) system is designed based on IEEE 802.11ad standards by exploiting millimeter-wave (mmWave) bands to achieve extremely high data rates. Recently, IEEE 802.11bd and 3GPP NR-V2X technologies adopted new specifications for the next generation vehicle-to-everything (V2X) network with the ability to support mmWave bands. However, mmWave bands could be the solution for the high throughput and low latency. Still, the instability of blockages is a substantial challenge in mmWave bands, rendering mmWave ineffective in vehicular networks. Typically, technologies capable of operating at mmWave bands, such as IEEE 802.11ad, IEEE 802.11bd, NR-V2X, etc., share the same technical challenges due to the unique characteristics of the mmWave band. As a result, to achieve the aspirations of next generation connected mmWave V2X vehicles. This paper proposes novel classic, cooperative, and extension protocols for IEEE 802.11bd by enhancing IEEE 802.11ad. The proposed solution aims to mitigate some of the most common technical challenges associated with using mmWave bands in V2X networks, such as beam training overhead, link blockage, beam misalignment, limited coverage range, and delay. Simulation results demonstrate that the proposed approach effectively reduces the beam training overhead, achieves accurate beam alignment, increases the probability of line-of-sight (LOS), overcomes link blockage/misalignment, extends the coverage range, and achieves low latency. Further, the proposed enhancement achieves significantly higher performance against the conventional solution and shows more link stability despite continuous changes in the density of the vehicles.

INDEX TERMS mmWave V2X communication, offline HD map-based localization, relay nodes, beam acquisition, beam alignment, beamforming, links blockage, beam misalignment, coverage range, latency.

I. INTRODUCTION

Vehicle manufacturers are currently transitioning towards electrically autonomous vehicles, where vehicles are autonomous and independently driven [1]. Autonomous automobiles rely heavily on communication technology to interact with their surroundings [2]. Dedicated short-range communication (DSRC), standardized by IEEE 802.11p [3], and long-term evolution (LTE) cellular V2X (C-V2X), based on third-generation partnership project (3GPP) LTE under release 14 [4] are the most common technologies used for the V2X systems based on licensed spectrum. Both radio access technologies were designed primarily to operate at the 5.9 GHz band. C-V2X and DSRC enable communication up to 1 km with data rates of 2-6 Mbps for DSRC and 100 Mbps for C-V2X. However, the study in [5] investigated why the

The associate editor coordinating the review of this manuscript and approving it for publication was Marco Martalo.

DSRC and 4G cellular systems are insufficient for supporting high data rates, low latency, and sharing raw sensor data on a large scale for future connected vehicles. Hence, researchers in [5] proposed three possible ways to exploit mmWave in future vehicular wireless systems, namely 5G cellular, a modified version of IEEE 802.11ad, or a dedicated new standard. Furthermore, the authors found that side information derived from out-of-coverage sensors is a crucial component of mmWave V2X systems. As a result, several studies indicate that more wireless resources are urgently needed to meet the increasing demands of the next-generation cellular and V2X systems [4], [5], [6], [7], [8], [9], [10], [11], [12], [13], [14]. The mmWave technology could be a potential solution to meet the extremely high bandwidth requirements by supporting the mmWave spectrum between (30-300 GHz) [6], [7], [8], [9], [10]. In response to these requirements, developments in technologies (e.g., IEEE 802.11, DSRC, and C-V2X) gave rise to technologies enhancing the performance and providing the ability to support mmWave bands, such as IEEE 802.11ad, IEEE 802.11bd, and 3GPP NR-V2X [6], [8], [11], [12], [13], [14], [15].

In this regard, IEEE 802.11ad is the wireless local area networks (WLANs) standard introduced as an amendment to IEEE 802.11 [16]. The protocol extends the operation of Wi-Fi networks to address the mmWave spectrum through new features at the medium access control (MAC) layer and physical (PHY) layer with the capability of supporting multiple gigabit wireless gigabit alliance (WiGig) [17]. Interestingly, WIGig has been developed based on the IEEE 802.11ad and IEEE 802.11ay standards and is dedicated to developing and enhancing wireless personal and WLANs in the 60 GHz band with backward compatibility of 2.4G Hz and 5 GHz with the ability to handle about 7 Gbps [16], [17], [18], [19], [20]. The use of IEEE 802.11ad to support multi-gigabit wireless vehicular communications has been investigated and evaluated in several studies [21], [22], [23], [24], but challenges associated with using the mmWave technology persist [21], [23]. Accordingly, to achieve robust and reliable IEEE 802.11ad-based mmWave vehicular communication, challenges related to using the mmWave technology need to be addressed, including beam training overhead, frequent link blockage, beam misalignment, short communication range, delay, and unstable connectivity [21], [22], [23], [24], [25], [26].

Therefore, to cope with these challenges, we provide an overview and an illustrative example of the most common technical challenges that need to be addressed in order to realize a robust and reliable mmWave V2X system.

Among the above challenges, beam alignment and beamforming are among the most common technical challenges that need to be addressed associated with the usage of mmWave spectrum in IEEE 802.11ad in particular, and mmWave V2X technology in general [21], [22], [23], [24], [26], [27], [28], [29]. Notably, beamforming and directional transmission are essential components in mmWave systems to compensate for the high path loss and to maximize beamforming gains [22], [30], [31]. In the initial beam alignment, to establish the mmWave link, the transmitter and receiver should align their beams. In this context, establishing perfect beam alignment requires prior knowledge of channel information, for instance, angle-of-arrival (AoA) and the angle-of-departure (AoD); however, without channel knowledge, most existing beam training methods rely on exhaustive beam search (EBS) where the transmitter and receiver scan all possible angular space, for all $360^\circ \times 360^\circ$ beam pairs in order to obtain the optimal beam pairs [17], [18]. Unfortunately, these solutions are constrained by vehicle speed in addition to obstructions [30], [32]. Furthermore, the delay in implementing exhaustive beam sweeping is an additional challenge due to the large number of beam candidates that need to be searched [29].

Fig. 1 (a) shows an illustrative example of beam alignment-based IEEE 802.11ad mmWave V2V. As demonstrated in Fig. 1 (a), through the initial beam alignment, the source vehicle (SV) and the intended vehicle (IV) should scan all possible beam directions to find the optimal beam pairing. Nevertheless, such a method may take several milliseconds [32]. While Fig. 1 (b) shows an illustrative example of a mmWave V2X network topology and signal propagation and demonstrates the IEEE 802.11ad challenges associated with link blockage, high path loss, and low signal penetration. Accordingly, several studies have indicated that blockage by surrounding vehicles or obstacles can be a significant challenge in mmWave systems due to the low penetration and high path loss in free space [22], [25], [26], [33]. Fig. 1 (b), illustrates LOS signaling and link blockage in a dense urban environment based on different vehicle sizes and types where SV can communicate with V3, V4, V5, V9, and V10 over the LOS link. In contrast, the LOS link between the SV and V2, V6, V7, and V8 is blocked by neighboring vehicles (NVs). In the same context, the short communication range of mmWave systems is another technical challenge associated with IEEE 802.11ad and other mmWave V2X technologies. According to [26], in a WiGig system, when the average throughput is above 1 Gbps, the average transmission range is about 20 m in outdoor environments. Therefore, the IV could easily get out of the SV coverage area by moving a few meters. As a result, short communication transmissions may result in frequent disconnected and out-of-coverage scenarios. As depicted in Fig. 1 (b), despite the short distances between the SV and NVs V2, V6, V7, and V8, which is approximately a few meters, however, LOS links between them are blocked by adjacent vehicles V3, V4, V5, V9, and V10. Along with the previous challenges, Fig. 1 (c) illustrates short transmission range problems where the IV is out of coverage of the SV in a range over 200 m, or the IV may disconnect by moving a short distance away from the SV, resulting in the SV being unable to send data packets (DP) to the IV. Beam misalignment caused by surrounding moving vehicles is a further challenge that needs to be addressed by vehicular communication-based IEEE 802.11ad. In IEEE 802.11ad, although initial beam alignment has been successfully established, the combination

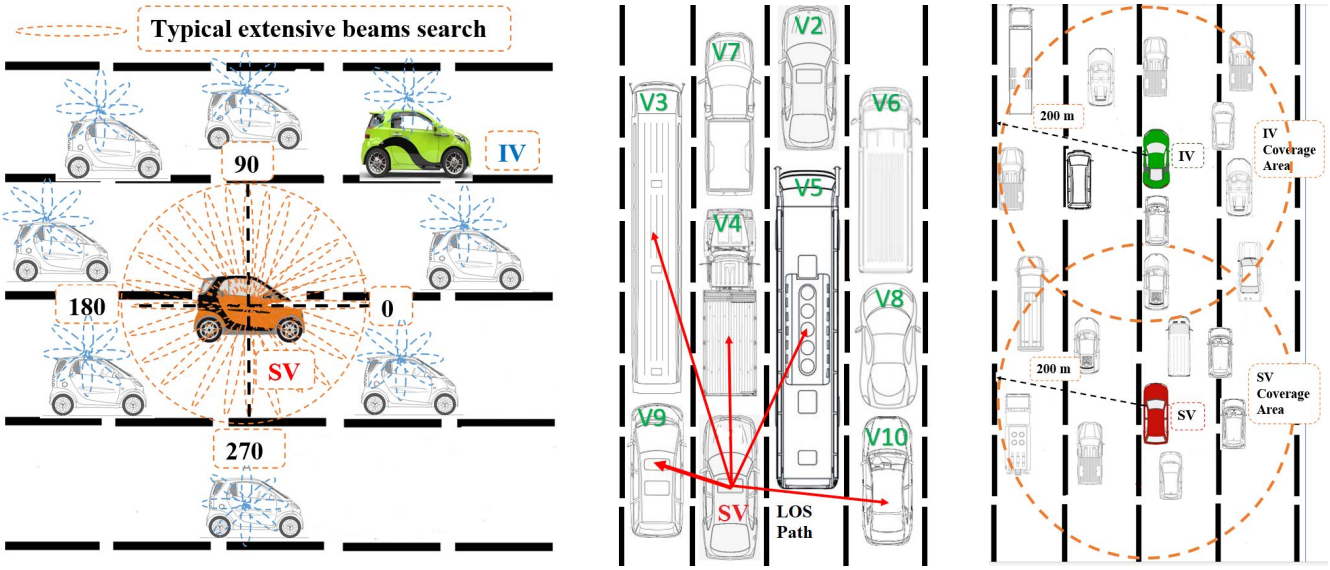

(a) MmWave V2V beam training through exhaustive beam searches.

(b) MmWave V2V channel propagation.

(c) Insufficient coverage range.

FIGURE 1. **Illustrative examples of common technical challenges associated with mmWave vehicular communication.**

of high vehicle mobility and narrow beams results in frequent beam misalignment [22], [30]. Thus, in order to re-establish the link, the two nodes need to search through all possible antenna beam configurations to establish the connection again, which results in additional delay and overhead [24]. The final problem outlined in this paper is the impact of delay, whether caused by the challenges discussed above or by scheduling schemes based on the request-to-send (RTS)/clear-to-send (CTS) handshaking mechanism [21]. In fact, low latency is crucial for ensuring high reliability and better performance [11], [13], [22]. Therefore, this paper briefly highlights some causes of end-to-end delays and then offers solutions.

In this regard, in order to improve wireless network capacity, and system performance, both 3GPP NR-V2X [13] and IEEE 802.11bd [11] are designed to incorporate interoperability of conventional frequencies below sub-6 GHz alongside mmWave bands. The 3GPP has published its release 16, which features the first V2X standard based on the 5G new radio (NR) air interface [13]. The aim of designing the NR-V2X is not to replace the LTE C-V2X, but to complement it with support for use cases that the LTE C-V2X cannot meet, such as high reliability and low latency [15]. High reliability and low latency, however, require a large amount of radio bandwidth [14]. To this end, the NR-V2X features capability for operation at two frequency ranges, FR1, under sub-6 GHz, and FR2, for the mmWave bands [13]. Also, the developments in DSRC resulted in the development of the task group (TGbd) IEEE 802.11bd created to replace the IEEE 802.11p, with the PHY layer offering up to 40 MHz channel bandwidth and the flexibility to support sub-6 GHz and, optionally, in the frequency range from 57 GHz to 71 [11], [12]. However, to the best of our knowledge, IEEE has not yet published specifications for mmWaves bands, except for a proposal to migrate portions of the MAC and PHY layers from IEEE 802.11ad/ IEEE 802.11ay [11]. Accordingly, the basis for the IEEE 802.11bd design relies on existing IEEE 802.11 standards and associated IEEE 802.11ad/ IEEE 802.11ay [12]. Thus, there is an open discussion about how to overcome the technical challenges of exploiting the mmWaves spectrum in IEEE 802.11bd [5].

Even though current existing mmWave vehicular technologies vary, such as IEEE 802.11ad, IEEE 802.11bd, NR-V2X, etc., their whole protocol stack challenges may remain the same due to the unique characteristics of mmWave bands [2], [15], [21], [22], [23], [24], [25], [28], [29]. Consequently, a successful protocol development to solve such challenges is essential for IEEE 802.11bd for the possible use of mmWave V2X communication and as a complement to 3GPP NR-V2X.

A. RELATED WORK

We classified the literature into two research trend categories. In the first category, in order to simplify and speed up adaptive channel estimation and beamforming, researchers in [34] provided that a location-aided beamforming strategy can significantly speed up initial access. While Wang *et al.* in [35] proposed a Low-complexity beam searching and beam selection approach by exploiting the angle information extracted from the beam codewords of the previous serving base station (BS) to minimize the size of the beam searching space of the target BS. To further minimize the number of beams to search and to reduce the beam alignment overhead, the authors in [36] exploited user equipment (UE) locations and potential reflection points. On the other hand, to mitigate

beam misalignment problems and reduce the beamforming overhead. Ioannis et al in [37], developed a smart motion-prediction beam alignment that exploits the broadcast information to estimate the vehicle's position and predict its motion. In the same context, to reduce the excessive complexity and obtain the lowest training latency of exhaustive beam search schemes based on IEEE 802.11ad/ay protocols, the authors designed a new transmission frame structure that adjusts a small number of training beams and frames [35].

The second category is latency and reliability of mmWave V2V networks under relay selections as well as link blockage avoidance [38], [39], [40], [41]. Based on mmWave signal propagation, network topology, and traffic density, in [38], the authors exploited the location information of vehicles and the adjacent distance to improve the performance of mmWave V2V multi-hop transmission latency and reliability. In order to minimize the effects of link blockage, LV *et al.* in [39] proposed blockage avoidance and optimal relay selection scheme-based mmWave V2V multi-hop sensor data dissemination, which allows for faster dissemination and minimizes transmission delays by using vehicle positions and utility functions. Along these lines, the literature in [40] proposed the proper selection of the next-hop relay nodes in high-density networks. This research develops a hybrid relay node selection by exploiting the features of message dissemination, including message accessibility, delay, and bandwidth. In order to improve outage probability and average total rate performance, the reference in [41] proposed using multi-relays, where an unlimited number of sources transmitted their messages to the target destinations through multi-relays, in which the relay decision relied on the measured SINR while planning tools are used to identify the best places for the relays. The study also demonstrates that the selection of relays significantly impacts system interference and that careful selection can enhance overall performance. In line with the research presented in [41], Liu *et al.* In [42] proposed using the resources of vehicles around the requested vehicles. Instead of requesting vehicles only to offload tasks to service vehicles as relay nodes. Therefore, request vehicles can use service vehicles as relay nodes to offload tasks beyond one-hop communication ranges. To achieve better performance of mmWave MAC for V2V communications and reduces the control overhead and delay. Reference [43] proposed to decouple the control and data planes utilizing a configuration of IEEE 802.11ad tailored to vehicular communications. By design a MAC using IEEE 802.11p for the control plane and IEEE 802.11ad for the data plane.

B. CONTRIBUTION

In this paper, we propose a novel solution for mmWave V2X communication protocols-based IEEE 802.11bd by enhancing IEEE 802.11ad in terms of

- Using offline location information (OLI) based on offline HD mapping-based localization for better beam alignment, fast beam acquisition, minimizing channel training overhead, and selecting the optimal relay vehicles (RVs) and dedicated vehicle stations (DVS) among addressed NVs.
- Using independent position estimation (IPE) and network topology lists (NTLs) to minimize end-to-end transmission delays and complexity.
- Using RVs to overcome link blockages and extend communication coverage.
- Using DVS for enhanced coverage and communication with vehicles beyond the coverage area.
- Using the diversity of selecting RVs to mitigate the effects of dynamic beam misalignment caused by moving vehicles and narrow beams.

We briefly discussed the challenges associated with using mmWave bands in V2X networks. Afterward, we offer possible solutions to overcome these challenges.

The authors propose a novel solution to overcome these challenges based on classic, cooperative, and extension protocols for IEEE 802.11bd to accommodate both (In/Out) cellular coverage scenarios.

In the classic protocol, two-stage algorithms were proposed to overcome the limitations of the beam-sweeping-based beam alignment method and enhance the beam alignment performance of mmWave V2V networks under different scenarios. In the first stage, a location-aided beamforming strategy is employed to narrow the beam search space of the target. While in the second stage, only the narrow beam search space is scanned to find beam pairings with the highest received signal strength (RSS).

In the cooperative protocol, we propose a multi-hop cooperation request (MHC-REQ) Beacon messages to overcome link blockage and enhance the communication range.

In the extension protocol, we propose a DVS approach to expand the communication coverage range of the mmWave V2X channel and enable communication with vehicles outside the coverage range.

In the overall protocol, we propose an accurate method for selecting RVs and DVS according to IPE and NTLs algorithms. Therefore, RVs and DVS are not selected randomly, but accurately based on their locations relative to SV, IV, NVs, and associated RSS. In this solution, the SV is responsible for choosing the most efficient RVs and DVS among the NVs candidates to maximize the likelihood of LOS in the current network topology.

In order to speed up decision-making and reduce end-to-end transmission delays, we propose IPEs and NTLs mechanisms. In IPE, we develop an accurate and independent location estimation algorithm by considering the vehicle status and the estimation error as inputs. Moreover, IPE categorizes vehicles based on their status into static and dynamic categories.

In the static status, the vehicle estimates its position independently based on the current position, speed $= 0$; delay before transmission start $= t_s$, and random estimation error e_r. While in the dynamic status, the vehicle predicts its location according to the current position, speed $=$ s, transmission

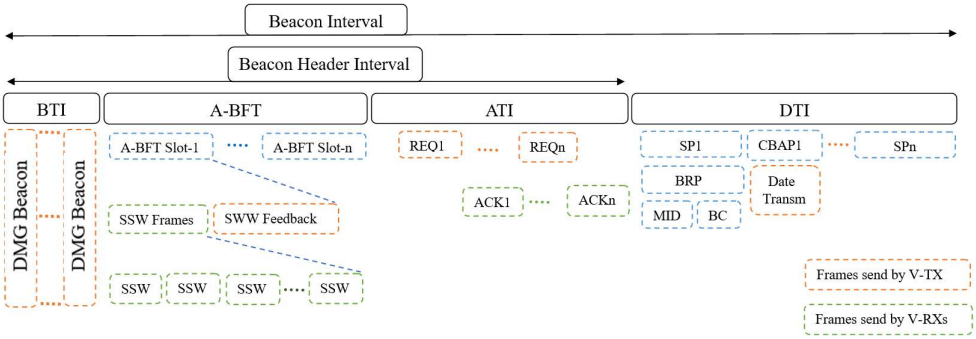

FIGURE 2. IEEE 802.11ad beacon interval structure and channel access.

delay t_s, and random estimation error e_r. However, OLI is used to estimate the current position.

The strength of the IPE method lies in the fact that each vehicle within the intended communication range can independently and accurately estimate its location and then send the location information to the SV. Therefore, we frame the solution as an accurate and fast collaborative teamwork process.

In NTLs, we propose a framework to facilitate and speed up the selection of an appropriate protocol among the three proposed, depending on the current network topology.

Finally, we propose a diverse RVs selection based on the proposed cooperative protocol to mitigate the potential of blocking some of the selected RVs during the data package delivery (DPD) mechanism. Therefore, diverse RVs can minimize the probability of frequent beam misalignments in a highly dynamic environment.

II. A BRIEF OVERVIEW OF THE IEEE 802.11AD STANDARD

A. IEEE 802.11ad- BASED mmWave V2X COMMUNICATION SYSTEM

The IEEE 802.11ad standard defines a common framework for multi-Gbps communications at 60 GHz and enhances the performance of V2X communications [16], [17]. In the mmWave bands, however, the link degrades more significantly than in the traditional under the sub-6 GHz band when passing through obstacles. A directional antenna is employed in IEEE 802.11ad to compensate for the high path loss observed in the mmWave bands.

The RTS/CTS handshaking mechanism is applied in an exhaustive sector-sweep manner during beacon exchange [21], [44]. Direct communication between the transmitter and receiver is possible if the connection link satisfies the transmission conditions. However, since the receiver location is unknown, exhaustive sector sweeping is used as part of the handshaking mechanism based on the quasi-omnidirectional to identify the optimal antenna sector, resulting in a high overhead and low link budget [20], [33]. In IEEE 802.11ad, beamforming is implemented during beacon intervals (BIs), and the channel access is divided into several BIs. As shown in Fig. 2, the BI consists of a beacon header interval (BHI) and a data transmission interval (DTI). Furthermore, the BHI comprises the beacon transmission interval (BTI), association beamforming training (A-BFT), and announcement transmission interval (ATI) [16], [43]. The (Bis) in IEEE 802.11ad is divided into several sub-intervals, as described in Fig. 2. [21], [45], [46], [47], [48]:

- Beacon transmission interval (BTI): In this sub-interval, the transmitter transmits DMG beacon frames across different antenna sectors to announce the network.
- Association beamforming training (A-BFT): In this sub-interval, beamforming is performed between the transmitter and responder by using a headshake mechanism.
- Announcement transmission interval (ATI): In this sub-interval, the transmitter and responder are managed and transmitted by the exchanged (REQ) and (ACK) frames.
- Data transmission interval (ATI): In this sub-interval, the contention-based access period (CBAP) and scheduled service period (SP) are exchanged between the transmitter and the responder for data transmission.

B. mmWave SYSTEM BEAM ALIGNMENT

In mmWave systems, antenna beamforming is employed at the transmitter and the receiver with the precise alignment of the beams for establishing a reliable and highly directional transmission link. However, quick beam pairs and low-complexity beam alignment are essential components for reliable mmWave V2X networks. The IEEE 802.11ad standard defines the so-called exhaustive beam sweeping, in which beams are scanned sequentially and evaluated to determine the optimal alignment beam pair [49]. Unfortunately, since location information is unknown, exhaustive beam sweeping at both transmitter and receiver leads to significant delays and associated communication overheads [25], [27], [46], [49].

III. SYSTEM MODEL

Based on an evolution of an IEEE 802.11p standard, the proposed system model enhances the IEEE 802.11ad, which

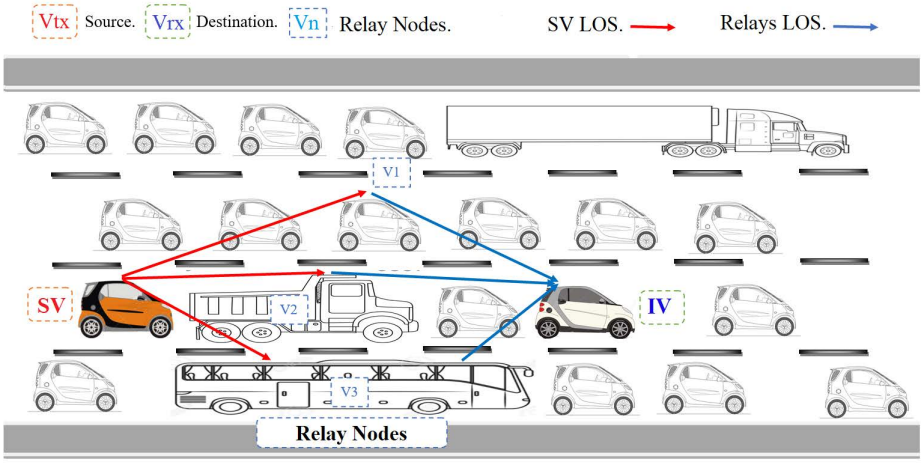

FIGURE 3. mmWave V2X network topology.

is one of the common V2X standards for DSRC. The key objective of our work is to overcome challenges faced by operating mmWave bands based on IEEE 802.11bd. In general, obstacles, mobility, and density are the main parameters affecting the mmWave V2X network topology and its performance. In the system model, we consider a mmWave V2V communication network where each vehicle is equipped with mmWave transceivers and operates with transmit power P_{tx}. Furthermore, the effective communication range is set to R_d. Those vehicles within the range of communication of the SV can communicate directly with the SV if the RSS meets the transmission requirements.

Fig. 3, demonstrates an illustrative example of the proposed system model by incorporating different types and sizes of vehicles in proportion to realistic urban environments. In which N vehicles move in the same direction $V_N = V_1, V_2, V_3, V_4, ..., V_n$, where the SV is located behind the IV with a distance of d_x, and NVs are in the position of blocking the LOS link between SV and IV.

The proposed system model acknowledges that NVs may act as obstacles to the association of LOS between SV and IV, but at the same time, they may facilitate signal transmission. Therefore, if the LOS is blocked and the RSS falls below the predefined threshold, the SV must communicate with the IV through selected RVs. In order to provide reliable and timely communication between the SV and IV, RVs are carefully selected based on the IPE. Additionally, if the LOS signal is blocked and RVs have been assigned for message forwarding, only transmission from the SV to selected RVs, and then from RVs to the IV, is allowed. All other vehicles within the communication range not addressed by the SV remain silent. Upon receiving the message from the SV, the selected RVs transmit the received DP to the IV. Carrier-sense multiple access with collision avoidance (CSMA/CA) [50] can use for shared wireless channels across nodes in a network. Further, to mitigate interference, the SV sensors the channel, and refrains from sending packets over busy channels [51]. As soon as the channel becomes accessible for transmission, requests to send and clears to send are used to initiate data transmission. Vehicle detection and location information are critical components of the proposed solution that provide the system with the current local topology [30], [52], [53]. Overall, in the case of link blockage, the proposed protocol is appropriate for passing the signal to NVs following the same trajectory. We assume that the proposed protocol can specify where the vehicle of the intended recipient is located, and which of the NVs are closest to the IV to transmit the data packet (DP) [53]. By tagging the intended recipient's vehicle information with an awareness message, each vehicle in the group becomes aware of the IV. We also assume that each vehicle in the connection region can identify the SV and IV location and identify its location concerning NVs in the current network topology.

As shown in Fig. 3, despite the fact that the vehicles V_1, V_2, and V_3 are in a position that blocks the LOS signal between SV and IV, they are also located in places where they are highly likely to reach the IV via LOSs. Therefore, it will be more efficient to use obstruction vehicles as a (medium/relay) to achieve the desired LOS link. As shown in Fig. 3, SV selected the obstruction vehicles V_1, V_2, and V_3 as relays to transmit DP to the IV.

A. CHANNEL MODEL

A hybrid MIMO architecture is considered for the mmWave V2X system in order to reduce power consumption and achieve an inexpensive system architecture [46], [48], [54], [55], [56]. At the V_{tx} side, the signal is preceded using a hybrid beamforming vector, and the received signals are combined according to the hybrid combiner vector at the V_{rx} side. The vector $\boldsymbol{f}$ represents a hybrid precoder employed on the $V_[tx]$, while a hybrid combiner vector w combines the received signals at V_{rx}. According to [48] and [54], the received signal at time t in the vehicle is given by

$$\boldsymbol{Y} = \boldsymbol{w}^H \boldsymbol{H} \boldsymbol{f} \boldsymbol{S} + \boldsymbol{w}^H \boldsymbol{n} \tag{1}$$

We assumed each vehicle has the same antenna array and RF chains. Therefore, the communication channel matrix link $\boldsymbol{H}$ between the V_{tx} and V_{rx} can be exemplified as $\boldsymbol{H} \in \mathbb{C}^{N_{\text{tx}} \times N_{\text{rx}}}$, $\boldsymbol{f} = \mathbf{F}_{\text{RF}}\mathbf{f}_{\text{BB}}$ denotes the hybrid precoder, where $\mathbf{F}_{\text{RF}} \in \mathbb{C}^{N_{\text{tx}} \times L_{\text{tx}}}$ and $\mathbf{f}_{\text{BB}} \in \mathbb{C}^{L_{\text{TX}} \times 1}$ are RF and baseband precoder, respectively. Where $\boldsymbol{w} = \mathbf{W}_{\text{RF}}\mathbf{w}_{\text{BB}} \in \mathbb{C}^{N_{\text{rx}} \times 1}$ is the hybrid combiner vector with $\mathbf{W}_{\text{RF}} \in \mathbb{C}^{N_{\text{rx}} \times L_{\text{rx}}}$ and $\mathbf{w}_{\text{BB}} \in \mathbb{C}^{L_{\text{rx}} \times 1}$ are the RF and baseband combiner, respectively. $\boldsymbol{S}$ are the transmitted symbols, and $\boldsymbol{n}$ is the additive is white Gaussian noise.

The mmWave narrowband frequency-flat channel can be modeled by [55] and [56].

$$\boldsymbol{H} = \sqrt{\frac{N_{V_{rx}} N_{V_{tx}}}{\rho}} \sum_{l=1}^{L} \alpha_l \boldsymbol{a}_{V_{rx}}(\theta_l) \boldsymbol{a}^H_{V_{tx}}(\phi_l) \tag{2}$$

where $N_{V_{tx}}$ and $N_{V_{tx}}$ are the transmit and receive antenna arrays size, respectively. ρ is large-scale pathloss and L denotes the number of paths. $\boldsymbol{a}$ denotes the complex path gains of the l th path. $\boldsymbol{a}_{V_{rx}}(\theta_l)$ and $\boldsymbol{a}^H_{V_{tx}}(\phi_l)$ are the antenna array response vectors. The array response vectors at the transmitter and receiver can be formulated by

$$\begin{cases} \boldsymbol{a}_{V_{tx}}(\phi) = \dfrac{1}{\sqrt{N_{V_{tx}}}} \\ \quad \times \left[1, e^{j\frac{2\pi d}{\lambda}\cos\phi}, \cdots, e^{j(N_{V_{tx}}-1)\frac{2\pi d}{\lambda}\cos\phi}\right]^T, \\ \boldsymbol{a}_{V_{rx}}(\theta) = \dfrac{1}{\sqrt{N_{V_{rx}}}} \\ \quad \times \left[1, e^{j\frac{2\pi d}{\lambda}\cos\theta}, \cdots, e^{j(N_{V_{rx}}-1)\frac{2\pi d}{\lambda}\cos\theta}\right]^T, \end{cases} \tag{3}$$

IV. PPOPOSED SCHEME

A. VEHICLE LOCALIZATION BASED ON OFFLINE LOCATION INFORMATION (OLI)

The main components of connected and autonomous vehicles are positioning and sensors. These include radar, lidar, and cameras [5], [39], [57].

The global positioning system (GPS) and global navigation satellite system (GNSS) allow positioning and tracking; however, they cannot always provide accurate positioning, especially in urban environments with buildings, multipath, and signal obstructions [58], [59], [60].

Combining GNSS and inertial navigation (INS) systems can improve localization performance. Nevertheless, this technology cannot accurately detect the surrounding environment [60].

5G NR-V2X introduces opportunities for vehicular positioning and tracking based on the estimation of the angle of arrival (AoA), angle of departure (AoD), and time of arrival (ToA). Unfortunately, the multipath propagation of wireless signals in an urban environment result in parameter ambiguities [13], [61].

The simultaneous localization and mapping (SLAM) technique is defined to achieve accurate autonomous vehicle localization without using GNSS and real-time kinematics (RTK) but based on sensors such as cameras, radar, and lidar [62], [63]. Therefore, the perceived environment realized by the map representation is computed simultaneously for the given setting. However, SLAM-based sensor techniques require high computing power [63].

High-definition (HD) maps integrated with sensors are widely used to demonstrate the environment and aid in accurate localization [64], [65], [66], [67]. HD maps provide high-precision environmental features based on a real map. A key advantage of HD maps is their ability to provide precise navigation and localization out of cellular coverage. Therefore, Google, Apple, and HERE supply high-definition maps for autonomous vehicles such as Tesla's [65].

Previously built map technology can provide accurate vehicle locations without GNSS/GPS and is robust to changes in weather conditions. A unique feature of offline preloaded maps is their ability to operate in areas without coverage. However, since roads and places do not change quickly, regular offline mapping updates can occur when a vehicle enters a coverage area. Therefore, in this model, we aim to leverage the features of preloaded high-definition maps and automated vehicle sensors such as radar, lidar, lasers, and cameras to speed up adaptive channel estimation and beamforming in/out-of-coverage environments, so-called OLI. However, recent studies have relied on offline-built maps to solve the vehicle localization problem presented in [66] and [67].

Therefore, we aim to use offline-built maps and a multi-sensor fusion approach to estimate the vehicle pose concerning the map by performing a map-matching algorithm [68]. Thus, locating vehicles is possible by matching semantic features with existing maps. Subsequently, we intend to apply a cooperative localization protocol to V2V communications [69], which allows vehicles to exchange location information with surrounding vehicles for location estimation.

B. VEHICLE-BASED CURRENT STATUS

Our approach classifies vehicles into two categories: static and dynamic. Static vehicles, such as those stopped at a traffic light or on crowded streets, whereas dynamic vehicles are vehicles that are in continuous movement. For a precise location estimation, it is necessary to consider the vehicle's status. Accordingly, if the vehicle is in static status, the location estimation is derived from the current OLI, speed $= 0$, and the linear ratio of the normal static error. In dynamic status, accurate location estimation relies on the current OLI, current speed, and delay to start transmission, in addition to the proportion of normal dynamic error.

In static status, the estimated vehicle position equation is given by $V_{\text{S}} \sim V_{\text{Curr}} + \log\mathcal{N}(\mu, \sigma_s^2)$. In dynamic status, the estimated position of the vehicle is computed according to, $V_{\text{D}} \sim V_{\text{Curr}} + V_{\text{Pre}} + \log\mathcal{N}(\mu, \sigma_d^2)$, where V_{Curr} represents the current position of the vehicles based on offline HD map-based localization, $\log\mathcal{N}(\mu, \sigma_s^2)$ denotes the normal static error, V_{Pre} indicates the predicted position based on current speed and delay to start transmission, and $\log\mathcal{N}(\mu, \sigma_d^2)$ is

the normal dynamic error. /*mu* and /*sigma* are the mean and standard deviation of the normal distribution, respectively.

C. INDEPENDENTLY POSITION ESTIMATION (IPE)

Fast selection of optimal relays and beams relies heavily on a collaborative approach to exchange a set of information between vehicles within the range of communication. Accurate and fast estimation of vehicle location parameters is a critical component of network topology.

In our solution, once the vehicles have successfully received location requests from the SV, each vehicle estimates its current location independently based on static and dynamic statuses and associated factors.

Vehicles that successfully estimate their position send their position estimation information to the SV. However, independent location estimations can help reduce the complexity of position estimation at the SV and minimize end-to-end transmission delays.

D. RE-UPDATE OLI AND IPE

Due to the rapid changes in the local topology of the vehicle environment, a continuous update of the surrounding environment information is necessary. However, GPS information for updating the local topology in vehicular environments has been investigated [70]. This approach proposes re-updating OLI and IPE frequently. Frequent updates of the local topology of each vehicle in the connection group are vital for obtaining precise vehicle locations over time. The OLI is updated based on the current vehicle position in the network topology, whereas the IPE is updated based on the current OLI and vehicle status. Accordingly, in our approach, we assumed that all vehicles in the network topology were able to update their OLI and IPE frequently every second.

E. LOCATION INFORMATION AIDED CHANNEL ESTIMATION

Beam-alignment methods assess the beam combinations of each vehicle before transmitting data, and the link is established based on the beam pair that achieves the highest reference signal receive power (RSRP) [71].

A codebook-based analog beamforming method has been proposed to simplify the configuration and alignment of arrays. However, the set of predefined beams in the codebook requires unacceptably high latency plus overhead [72]. Due to the uncertainty of target location information, achieving rapid beamforming is challenging in a mobile environment. Conventional beam sweeping solutions have a high overhead since beamforming occurs via a traditional exhaustive beam search, which takes several milliseconds [27], [28], [71].

Typically, estimating receiver location information can significantly accelerate beam sweeping and initial access time, which further reduces beamforming overhead [34], [34], [34], [35], [36].

Therefore, we aim to exploit location information derived from sensors effortlessly to reduce the required beam search space in/out-of-coverage environments. However, optimizing estimation performance metrics could be achieved if prior vehicle position information is available.

In our approach, position-aided beam training can be summarized as follows: Beam training starts with the SV sending the training request IPE-REQ beacon message to NVs. Responders then respond with an acknowledgment containing their position information and IPE-Vn beacon messages. The IPE obtained from vehicles can be converted into information on angle-position coordinates. Subsequently, the SV exploits position information to determine a narrow list of optimal beam directions and alignment accuracy. Next, the transmitter scans the selected narrow angle on the receiver side to obtain the optimal beam pair. Then the optimal weights and adjusting the magnitude and phase of the signals are determined. These weights are then applied to the transmit signal to direct the beams towards the targets [73]. However, the training data for a limited budget include the position, the orientation, and the RSS measurements for all combinations. Therefore, the proposed solution meets its design objectives by achieving precise beam alignment and accelerating optimal beams coupled with the highest RSS.

F. PROPOSED T_x, R_x ARCHITECTURE WITH SIDE OFFLINE LOCALIZATION INFORMATION

The perspective of the design objectives in this section is to reduce search space by leveraging location information. We formulate the possible AoA/AoD ranges as a function of transmitter and receiver location information coordinates. The position matrix $\mathbf{P} \in \mathbb{R}^{2\times N}$ contains the two-dimensional location coordinates, where $\mathbf{P}_n = [\mathbf{p}_{x_n}, \mathbf{p}_{y_n}]^{\mathrm{T}}$ denotes the location information coordinates of the nodes. According to the studies in [35] and [36], the estimated location information can speed up beam alignment and reduce the search time as follows:

Let's assume $\mathbf{P}_i$ refers to the location information matrix that contains the coordinate information of the transmitter and receiver, and n is the number of the node.

$$\begin{cases} \boldsymbol{P}_i = [\mathbf{p}_0, \mathbf{p}_1, \ldots, \mathbf{p}_{N-1}], \\ n = [0, \ldots, N-1], \end{cases} \tag{4}$$

where

$$\boldsymbol{P}_0 = \begin{cases} \mathbf{P}_{\mathrm{TX}} & \text{for } i = \text{RX}, \\ \mathbf{P}_{\mathrm{RX}} & \text{for } i = \text{TX}, \end{cases} \tag{5}$$

The current location information $\mathbf{P}_0$ can be referred to as current transmitter location information $\mathbf{p}_{TX}$ when the receiver observer, and current receiver location information $\mathbf{p}_{RX}$ when the transmitter observer. Moreover, the independent location information model of the transmitter and receiver can be formulated in the following manner:

$$\begin{cases} \hat{\boldsymbol{P}}_{\mathrm{TX}} = \mathbf{P}_{\mathrm{TX}} + \mathbf{E}_{\mathrm{TX}}, \\ \hat{\boldsymbol{P}}_{\mathrm{RX}} = \mathbf{P}_{\mathrm{RX}} + \mathbf{E}_{\mathrm{RX}}, \end{cases} \tag{6}$$

where $\mathbf{P}_{\mathrm{TX}}$ and $\mathbf{P}_{\mathrm{RX}}$ refers to the current location estimation or location prediction between the transmitter and receiver

based on the current status (static/dynamic). $\mathbf{E}_{\mathrm{TX}}$ and $\mathbf{E}_{\mathrm{RX}}$ are the matrices that indicate the random location estimation errors associated with given x and y coordinates for the transmitter and receiver, respectively [74].

$$\begin{cases} \boldsymbol{E}_{\mathrm{TX}} = [\mathbf{e}_0^{\mathrm{TX}}, \mathbf{e}_{1,}^{\mathrm{TX}}, \ldots, \mathbf{e}_{N-1}^{\mathrm{TX}}], \\ \boldsymbol{E}_{\mathrm{RX}} = [\mathbf{e}_0^{\mathrm{RX}}, \mathbf{e}_{1,}^{\mathrm{RX}} \ldots, \mathbf{e}_{N-1}^{\mathrm{RX}}], \end{cases} \tag{7}$$

The estimated angle in the Euclidean plane between the x-axis and the point (x, y) for the transmitter and receiver is given by

$$\begin{cases} \alpha_{TX} = \left(\dfrac{\hat{x}_n^{\mathrm{TX}} - \hat{x}_{\mathrm{TX}}}{\hat{y}_n^{\mathrm{TX}} - \hat{y}_{\mathrm{TX}}} \right), \\ \alpha_{RX} = \left(\dfrac{\hat{x}_n^{\mathrm{RX}} - \hat{x}_{\mathrm{RX}}}{\hat{y}_n^{\mathrm{RX}} - \hat{y}_{\mathrm{RX}}} \right), \end{cases} \tag{8}$$

where $\hat{x}_{\mathrm{TX}}$ and $\hat{y}_{\mathrm{TX}}$ are the estimated x and y coordinates of the transmitter due to its uncertain position. Similarly, $\hat{x}_{\mathrm{RX}}$ and $\hat{y}_{\mathrm{RX}}$ are the estimated x and y coordinates of the receiver over its uncertain position. Based on estimated location information at the transmitter and receiver, the associated AOD/AOA can be calculated as follows:

$$\begin{cases} \hat{\phi}_n = \dfrac{\pi}{2} - \arctan(\alpha_{TX}), \\ \hat{\theta}_n = \dfrac{\pi}{2} - \arctan(\alpha_{RX}), \end{cases} \tag{9}$$

Therefore, based on the location information available at the receiver, the AOA of the m-th path to the receiver can be evaluated.

Where $\hat{x}_{RX}$ and $\hat{y}_{RX}$ are the estimated x and y coordinates of the receiver since its position is uncertain.

The following are the estimated distances between the transmitter and receiver

$$\begin{cases} \hat{d}_n^{\mathrm{TX}} = \sqrt{(x_{\mathrm{TX}} - \hat{x}_n^{\mathrm{TX}})^2 - (y_{\mathrm{TX}} - \hat{y}_n^{\mathrm{TX}})^2}, \\ \hat{d}_n^{\mathrm{RX}} = \sqrt{(\hat{x}_{\mathrm{RX}} - \hat{x}_n^{\mathrm{RX}})^2 - (\hat{y}_{\mathrm{RX}} - \hat{y}_n^{\mathrm{RX}})^2}, \end{cases} \tag{10}$$

The proposed coordinate beam alignment algorithm uses estimated location information and estimated location information error. However, the transmitter and receiver jointly search the beam vectors in a narrow beam search area during the beam alignment phase. The transmitter selects the beam steering vector $S_T X_n$ that corresponds to the obtained AOD and transmits it to the receiver, after which the receiver selects a combining vector $C_R X_n$ that is nearest to the estimated AOA, which can be calculated as follows:

$$\begin{cases} \boldsymbol{S_T X_n} = f_{\mathrm{TX}}(\hat{\phi}_n), \\ \boldsymbol{C_R X_n} = f_{\mathrm{RX}}(\hat{\theta}_n), \end{cases} \tag{11}$$

It is worth noting that the extremely high accuracy of beam search angle estimation is not essential for our method, as shown in Fig. 4 (a). In the first step, the aim is only to narrow the angle of the beam search. In the next step, the very accurate transmission angle is obtained by performing a sweeping mechanism through a predefined narrow search angle. Thus, the narrow-predefined search angle and the physical angle have some disparity.

As depicted in Fig. 4 (a), the orange beams represent conventional exhaustive beam search, while the blue beams indicate the pre-selected narrow search angle, and the red beam denotes the selected beam.

G. BEACONS DEFINITIONS

In this section, we outline an overview of the types of beacon messages exchanged during the proposed channel access period as follows:

- Independent position estimation (IPE), low latency beacon messages are exchanged and updated periodically between the SV and NVs. There are two kinds of IPE beacon messages: (1) Independent position estimation request (IPE-REQ) is sent within the DMG beacons during the initial access in one packet by SV. (IPE -REQ) carries information such as IDs, SV IPE, IPE-REQs, etc.

(2) Independent position estimation-feedback (IPE-feedback), low-latency messages containing IPE information, transmitted in a single packet with SSW frames by NVs.

- Multi-hop cooperative (MHC) Beacon messages are conditional, low-latency messages sent by SV. The MHC carries information concerning the SV, IV, and selected RVs such as MAC, position, identification ID, SP access period, etc. However, there are three kinds of MHC beacon messages.

(1) Multi-hop cooperative-Request (MHC-REQ) Beacon messages are sent by the SV to the selected RVs notifying them of the desire to transfer the DP to the IV using the cooperative protocol.

(2) Multi-hop cooperative-Feedback (MHC-Feedback) Beacon messages are sent by selected RVs to the SV to report the ability to send the DP and start sending the DP.

(3) Multi-hop cooperative-Acknowledge (MHC-ACK) Beacon messages are transmitted by selected RVs to the SV to acknowledge that the DP transmission is complete.

- Extending the communication range (ECR) Beacon messages are conditional, low-latency messages sent by SV. The ECR carries information concerning the SV, IV, and selected DVS, such as MAC, position, identification ID, SP access period, control packet, type of transmission protocol, etc. However, there are three kinds of ECR beacon messages.

(1) Extending the communication range-Request (ECR-REQ) Beacon messages are sent by the SV to the selected DVS informing of the desire to transfer the DP to the IV using the extension protocol.

(2) Extending the communication range-Feedback (ECR-Feedback) Beacon messages are sent by selected DVS to the SV to inform the possibility of DP transmission and start sending the DP.

(3) Extending the communication range-Acknowledge (ECR-ACK) Beacon messages are sent from the selected DVS to the SV to acknowledge the completion of the DP transmission.

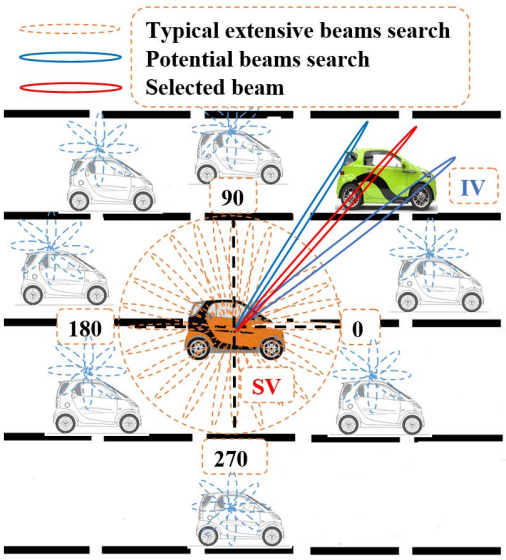

(a) Illustrative example of the SV searching for an optimal beam pair with the IV by scanning a predefined, narrow search angle.

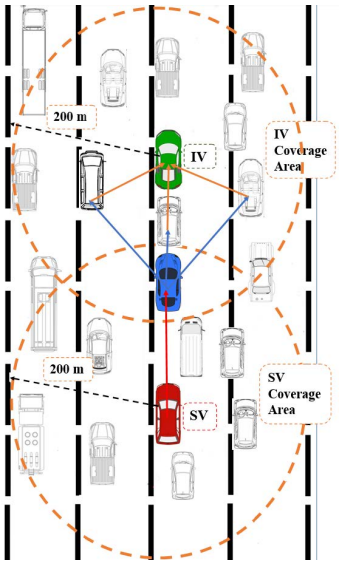

(b) This example illustrates the SV's ability to transmit DP to the IV out of the coverage area by selecting DVS.

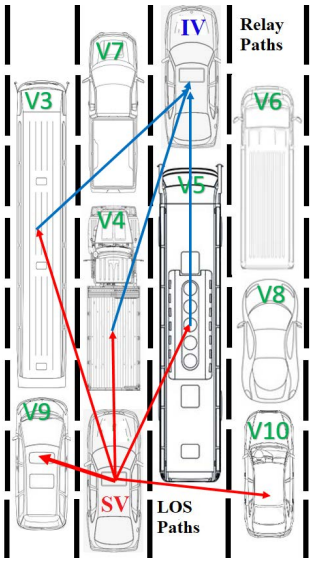

(c) Illustrative example of mmWave V2V signal propagation based on the diversity of RVs

FIGURE 4. **Illustrative examples of the proposed solutions.**

H. NETWORK TOPOLOGY LISTS (NTLs)

The NTLs indicate the vehicular network topology information in the current environment based on location and the corresponding RSS. The RSS measures the received signal strength of the reference signals within predefined thresholds. However, the RSS value of a single receiver antenna is recorded periodically during the measurement period.

In the initial phase of the beacons exchange, during the (BTI/A-BFT) access periods, as soon as the (DMG/IPE-REQ) and (SSW/IPE) Beacon frames exchange are completed, the SV generates NTLs immediately.

The NTLs consist of the classic list, cooperative list, and extension list in the following sequence:

(1) A classic list is used to store the IPE of the SV and IV in order to identify the narrow steering angle, locate configuration information from peer vehicles with its corresponding RSS, and store/map the best transmit and receive antenna sectors candidates based on the classic protocol.

(2) the cooperative list is used to store, map, and locate RV candidates with their corresponding RSS from NVs in the list.

(3) the extension list is used to store, map, and locate DVS candidates with their corresponding RSS and store the associated selected protocol for the final DPD mechanism.

Following the creation of the NTLs, the SV analyses and compares the information in the three lists in order to determine the type of protocol used for the DPD mechanism.

The SV selects one of the three lists of NTLs based on the availability of information in the lists and the order among the three lists.

For instance, assuming the information is available in all three lists simultaneously, the SV gives priority to the classic list, next to the cooperative list, and finally to the extension list sequentially.

It is worth noting that any of the NVs that have successfully received (DMG/ IPE-REQ) frames could be a candidate member of the three lists at once, depending on their position within the network topology.

However, each vehicle from the NVs can join the NTLs candidates if the following conditions are satisfied: (1) NVs that have successfully received (DMG/IPE-REQ) Beacon frames. (2) NVs that share the same range of communication with SV and IV. (3) NVs that successfully detect the existence of the IV within its communication range. (4) NVs that have the same trajectory as SV and IV. (5) NVs with the capability to identify the type of protocol used in the DPD mechanism.

NVs that have successfully met the requirements to join the NTLs are responsible for: (1) search for the IV within their coverage area, (2) determine its position relative to the SV and IV. (3) find the narrow beam angle towards IV, determine the corresponding RSS relative to SV/IV, and join the classic list. (4) select RVs candidates, determine the corresponding RSS relative to SV/IV, and join the cooperative list. (5) select DVS candidates, determine the corresponding RSS relative to SV/IV, specify a final DPD mechanism among broadcast, classic, or cooperative protocols, and join the extension list.

Addressed NVs can join all or some of the list based on their position in the current network topology, after which the SV adopts one of the proposed transmission protocols based on a list of criteria.

I. COMMUNICATION RANGE EXTENSION

In vehicular networks, communication range relies on several parameters (e.g., frequency band, transmission power, obstacles, and environment). DSRC can theoretically achieve a communication range of 1000 meters on the freeway under

sub-6 GHz. Unfortunately, dynamic physical obstructions in urban environments can reduce the communication range to less than 100 meters [75].

Since path loss varies inversely with wavelength, mmWave systems are subject to higher attenuation, thus having a smaller transmission range than conventional technologies [21], [22]. The mmWave communication channels are theoretically possible at ranges less than 200 m in most measured links [8]. However, in dense urban environments, the actual transmission range of mmWave channels is well below 200 meters.

We propose an enhanced solution for extending the transmission range of the mmWave V2X channel in actual dense environments by allowing the SV to communicate with the IV through DVS beyond its coverage, as shown in Fig. 4 (b).

Specifically, the proposed protocol is divided into two stages, one for listing DVS candidates and the other for selecting the best DVS from among lists. A DVS is chosen precisely midway between the SV and IV communication range to manage and transmit the DP simultaneously to the further selected RVs in the next hop for the final DPD mechanism, as shown in Fig. 4 (b). However, the final DPD-based DVS is restricted to broadcast, classic, and cooperative protocols. Thus, the DVS cannot use the expansion protocol for the DPD mechanism.

If a DVS uses the classic protocol for the final DPD, then the DVS steers its beam toward the IV directly based on IPE.

In the case of cooperative protocols, the selected RVs of the second network synchronize the transmitting time and frequency according to a control packet transmitted by the DVS.

The control packets are used to synchronize and trigger the transmitting time of RVs on one hop if the cooperative protocol is employed. Once the control packet is received successfully at RVs, the DP containing the IV address and encoding is transmitted simultaneously.

J. DIVERSITY RV/DVS VEHICLES

Cooperative and extension protocols may fail due to frequent changes in the location of the RV/DVS caused by continuous movement in the vehicular environment. That results in the effect of so-called link misalignment or link re-establishment problems [30]. Therefore, to achieve high reliability and improve the performance of the mmWave V2X channel, we proposed a diversity in the selection of RV/DVS based on the IPE and NTLs. As shown in Fig. 4 (c), the SV can choose more than one RV depending on the location of the RV relative to the SV and IV in the current network topology. In general, the diversity of RV/DVS aims to reduce the effects of dynamic obstacles and address the potential for blocking some RVs/DVSs. As shown in Fig. 4 (c), the SV communicates with the IV through diverse RVs V3, V4, and V5. However, the SV can choose more than one RV/DVS from among RV/DVS candidates in NTLs.

K. LOW-LATENCY NETWORK

In this section, we propose a novel framework that blends IPE with an intelligent selection of RVs/DVS, along with selecting the appropriate protocol from among the three protocols based on current network topology to dynamically and efficiently pair vehicles, reduce the end-to-end latency, and increase the throughput. This is achieved by jointly considering IPE-based channel state information and NTLs-based automatic list selection when establishing a mmWave V2V channel. Therefore, considering its design objectives, the proposed low latency scheme is comprehensive and considers several factors that directly affect packet delivery latency, including location, beam alignment delay, feedback delay, blockages, density, beam misalignment, decision-making time, and beam coherence time. In summary, the low latency approach can be summarized as follows:

- With OLI, the beam searching space can be reduced, thus minimizing the beam alignment delay.
- IPE allows vehicles to estimate their location independently and transmit IPE information to the SV. Therefore, the SV can reduce computational complexity by speeding up the needed time for perceiving the surrounding environment, locating obstacles concerning the IV, and making decisions based on choosing RVs/DVSs.
- Based on NTLs, the SV can reduce delays caused by the make-decision time of selecting the appropriate protocol for the current network topology.
- Based on the cooperative protocol, the SV can reduce the delay associated with link blockage and repeat the link re-establishment mechanism.
- Based on the extension protocol, the SV can reduce the delay associated with vehicles frequently leaving coverage areas.
- Based on the diversity of RVs/DVSs, SV can reduce delays associated with frequent beam misalignments.

V. PROPOSED PROTOCOL

The proposed solution introduces three access protocols: classic, cooperative, and extension protocols. SV selects the type of access protocol based on the availability of information in NTLs, and the order of the list in NTLs. Whenever the SV wants to transmit DP to an IV, it initiates by broadcasting (DMG/IPE-REQ) Beacon frames to all NVs. However, (DMG/IPE-REQ) beacon frames are sent across different antenna sectors in order to (1) announce the network, (2) request IPE, (3) provide synchronization, (4) transmit BI structure information, (5) transmit SV/IV information, (6) provide training, and (7) announce the starting of creating NTLs.

An overview of the classic, cooperative, and extension protocols is outlined below:

Classic protocol: In this protocol, we assume there are no obstacles between the SV and IV, and the RSS measurement meets the predefined threshold. As a result, their channel is adequate for transmission. However, in all protocols, during

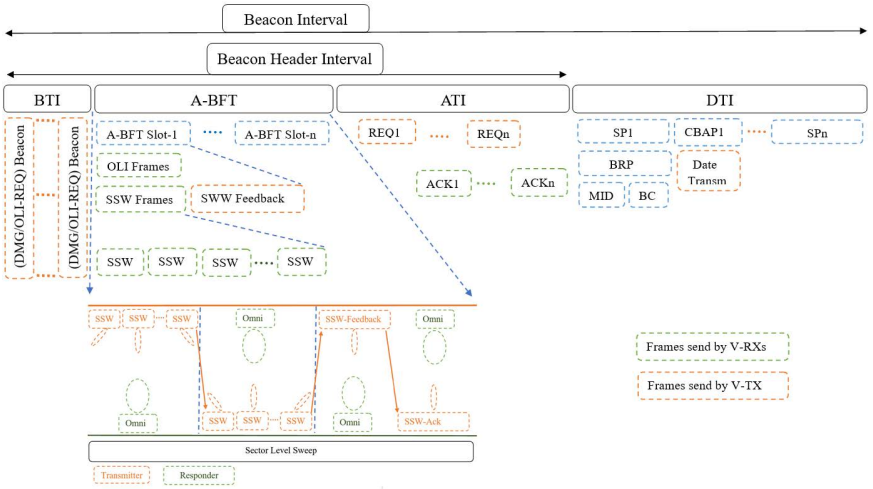

(a) Proposed classic pattern, beacon interval structure, and beamforming training.

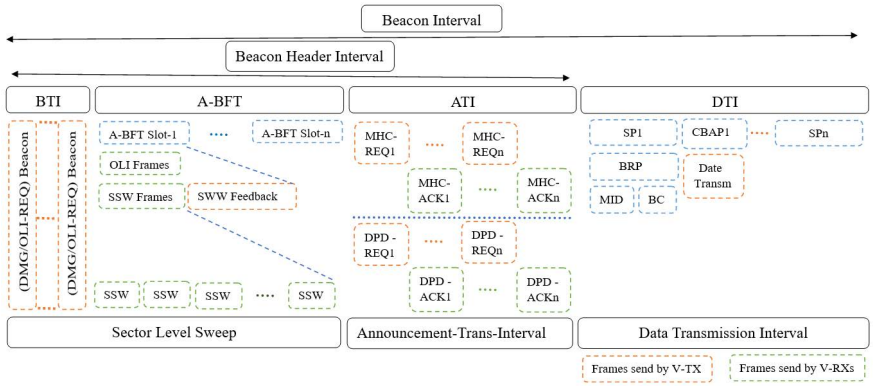

(b) Proposed cooperative and extension patterns, beacon interval structure, and channel access.

FIGURE 5. Proposed beacon interval structures.

initial communication, the SV transmits (DMG/IPE-REQ) Beacon frames from different antenna sectors to NVs, while NVs receive by a quasi-omnidirectional. NVs successfully addressed by (DMG /IPE-REQ) Beacon frames immediately respond to the SV by sending (SSW / IPE-n) frames. The exchanged beacon frames between them comprise MAC addresses, antenna sector identification, and a countdown (DOWN), among other information. Once the initial beacon message exchange is completed, the SV instantly creates classic, cooperative, and extension lists. However, none of the three lists record any information if the addressed NVs do not meet the requirements for membership. For instance, no data is recorded in the classic list if the received RSS level falls below the predefined threshold.

In contrast, if the RSS measurement exceeds or equals the predefined threshold, then the SV creates a classic list. Thus, the classic list information is used to establish channel access between the SV and IV, and then the classic protocol is applied for the DPD mechanism.

In this scenario, SV determines the narrow steering angle based on information in the classic list. The SV then scans the selected narrow angle and identifies the best transmit and receive antenna sectors according to the receiver address in the MAC header. Finally, the SV steers its beam toward the selected antenna sector.

As demonstrated in Fig. 5 (a), the SV transmits the SSW feedback frame to the IV after the SV selects the optimal antenna sectors. The IV uses the best sector to send the (SSW-ACK) frame to the SV. Once the SV successfully receives the (SSW-Ack) frame, the link establishment is complete, and the DP transmission begins. Upon completing the above steps, the DP is transmitted using the classic protocol, and the SV erases all data stored in NTLs.

Cooperative protocol: this protocol assumes obstacles have blocked the link between the SV and IV. Thus, the RSS level drops below the predefined threshold. As a result, no information will be available on the classic list. Therefore, the SV will switch to using the cooperative list, which is listed as a second list in the order of NTLs.

In the same manner as in the classic protocol, once the SV wants to transmit DP to the IV, the communication initiates by exchanging (DMG/IPE-REQ) and (SSW/IPE-n) Beacon

messages. Thus, classic, cooperative, and extension lists are created simultaneously.

A cooperative list contains information about RVs candidates, such as their location relative to SV/IV paired with their RSS, SSW, MAC, ID, IPE, etc.

If the SV chooses the cooperative protocol to send the DP, the SV then analyzes and compares the information in the cooperative list to select the most suitable RVs from the list of candidates.

The trade-off for selecting the best RVs from among the RV candidates is given to the candidate with the highest probability of LOS linking with the IV, as well as if its RSS level relative to SV is satisfied.

Once the optimal RVs are selected, the SV directs its beams towards the selected RVs over a narrow angle based on the IPE and transmits the (MHC-REQ) frames. The (MHC-REQ) frames carry various information such as IPE, ID, MAC address, transmission duration time, synchronization, and so on.

All NVs are aware of the transmission information between the SV and IV through the (MHC-REQ) frames. When the selected RVs successfully receive the (MHC-REQ) frame, they respond with the MHC-Feedback (MHC-FBCK) frame to the SV. The SV starts DP transmission after receiving the (MHC-FBCK) frame. Under the cooperative protocol, the SV can establish an MHC transmit link through selected RVs rather than using the direct path, which is blocked by obstacles. As soon as the SV aligns its beam toward the selected RVs, it begins transmitting a DP. Selected RVs can broadcast or direct their beams towards the IV over the IPE. Upon receipt of the DP by the RVs, the IV sends an acknowledgment (MHC-ACK) frame to the RVs to confirm receipt of the DP. RVs then forward the (MHC-ACK) frame to the SV. Once the (MHC-ACK) frame is received, the DP transmission is completed, and the SV erases the data stored in the NTLs.

Extension protocol, In this scenario, the IV is assumed to be out of the coverage of the SV. As a result, the SV cannot obtain any information about the IV. Therefore, the SV requests NVs to locate and provide information about the IV within their coverage area. Eventually, the SV selected and requested the DVSs to communicate and deliver the DP to the IV.

Similarly, upon completing an exchange of (DMG/IPE-REQ) and (SSW/IPE-n) Beacon messages, valuable information is gathered that enables the SV to choose the appropriate protocol for given network topology. However, the vehicle location within the network topology, corresponding RSS, NV candidate location relative to the SV and IV, and MAC addresses are essential components of the protocol selection mechanism.

Once the initial beacon message exchange is complete, NTLs are created instantly. Any NV addressed by (DMG/IPE-REQ) Beacon frames and could not locate the IV within its coverage range is out of competition and does not communicate with the SV. The SV sends the DP via an expansion protocol if the information is unavailable in both the classic and cooperative lists. Each NV can be a member of one or more lists simultaneously, depending on its position in the network topology and associated RSS.

However, SV uses the extension protocol when it cannot use the classic and cooperative protocols. After creating a DVS candidates list, the SV analyzes and compares the information in order to select the best candidate to be a DVS. However, the trade-off strategy that the SV uses for selection depends on the protocol used by the DVS candidate for the final DPD mechanism and the corresponding RSS. In this regard, the selection priority is given to candidates that adopt the classic protocol and then the cooperative protocol in conjunction with the corresponding RSS.

After the optimal DVS is chosen, the SV directs its beams toward the selected DVS using the IPE and starts to transmit the (ECR-REQ) frames. The (ECR-REQ) frames contain vital information regarding IPE, ID, MAC address, transmission time, synchronization, etc. The NVs are aware of the transmission information between the SV and IV over (ECR-REQ) frames. After the selected DVS receives the (ECR-REQ) frame, it responds by sending the (ECR-FBCK) frame to the SV to initiate a DP transmission. Using the selected DVS, the SV can establish the ECR transmission link with an IV that is out of coverage. The DVS can send DP to the IV via broadcast, classic or cooperative protocols. IV notifies DVS that the DP has been received by sending the (ECR-ACK) frame. Afterward, the DVS forwards the (MHC-ACK) frame to the SV. After a frame (ECR-ACK) is received, the DP transmission is completed, and SV deletes the data stored in NTLs. Extending protocols can avoid misalignment problems by selecting a diverse set of DVSs.

Across all proposed protocols, countdown (CDOWN), antenna sector ID, MAC address, and IPE are mandatory exchanged beacon messages. Meanwhile, MHC-REQ and ECR-REQ are conditional beacon messages.

Fig. 5 (a) and (b). illustrates an example of channel access and beacon intervals under the proposed scheme. Where (DMG/IPE-REQ) frames take place in the BTI interval, whereas A-BFT slot, association beamforming training, IPE, SSW frames, and SSW feedback take place in A-BFT intervals.

As depicted in Fig. 5 (a) and (b), BRP is performed in the DTI interval and consists of multiple sector IDs (MIDs), beam combining (BC), and beam refinement transactions (BRTs).

Following is a description of the proposed channel access and beacon interval as described in Fig. 5 (a) and (b):

Beacon Transmission Interval (BTI): As depicted in Fig. 5 (a) and (b), in the initiator sector-level sweep (SLS), DMG beacons are encapsulated within IPE-REQs frames in one packet with other information and then broadcast to NVs within the intended communication range.

Association Beamforming Training (A-BFT): As shown in Fig. 5 (a) and (b), in the A-BFT, the transmitter trains its antenna sectors to communicate with respondents based on received SSW frames associated with IPE. A-BFT uses

IPE while selecting an A-BFT slot to contend for the training opportunity based on sector sweep frames.

Announcement Transmission Interval (ATI): As illustrated in Fig. 5 (a) and (b), during the ATI access period, the SV manages the tire exchange process related to the pairing with the IV. The frames transmitted during the ATI access period are optional, such as (frame management, REQ, ACK, MHC-REQ, MHC-FBCK, MHC-ACK, ECR-REQ, ECR-FBCK, ECR-ACK, etc.). Consequently, ATI has indicated in the associated current (DMG/ IPE-REQ) Beacon frames.

Data Transmission Interval (DTI): As reported in Fig. 5 (a) and (b), DTI includes contention-based access periods (CBAPs) and scheduled service periods (SPs), which allow the SV and IV to exchange data frames. Furthermore, SP comprises a specific time interval intended for exclusive communication.

A. CHANNEL ACCESS AND BEAMFORMING TRAINING

Beamforming training is designed by training a bidirectional transmission frame to determine the optimal receiving and transmitting antenna sectors based on the received IPE. The transmitters and responders train their TX sectors during the sector-level sweep phase. The responders sent a training request along with its context information and the latest IPE to the SV. Thus, the SV recommends an optimal narrow beam sweep list to scan the responder antenna sector.

The sector-level sweep phase consisted of three parts:

1) Initiator Sector Sweep (ISS): ISS, is the initial step of BF, during the BTI period. The ISS sub-phase sends training (DMG/IPE-REQ) Beacon frames to the receiver comprising the sector ID associated with the antenna sectors and IPE request.

2) Responder Sector Sweep (RSS): RSS is the second sub-phase procedure in the BF training, which occurs during the A-BFT period. After successfully receiving the packets of (DMG/IPE-REQ) Beacon frames sent by the transmitter and based on the measured SNR for each received frame, the optimal sector ID of each associated ISS is determined by the transmitter.

3) Sector Sweep Feedback (SSW-FBCK): Once the transmitter has successfully transmitted its SSW frames, it transmits SSW-Feedback on the optimal transmission sector to the receiver. The transmitter selects the optimal beam pair based on the strength of the received signal on the receiver side. Upon completion of the SSW feedback, the responder sends the SSW ACK.

B. IEEE 802.11ad VS THE PROPOSED PROTOCOL

The objective of this section is to demonstrate the key advantages of the proposed solution and to point out the main differences between the proposal and the IEEE 802.11ad standards.

IEEE 802.11ad, in the BTI interval, the initiator transmits starting with DMG Beacon frames, whereas the proposed method initiator transmits starting with (DMG/IPE-REQ) Beacon frames. In IEEE 802.11ad, responders respond with SSW frames, while in the proposed solution, responders respond with SSW and associated IPE-n frames. As demonstrated in Fig. 2, IEEE 802.11ad does not support prior location information, while the proposed solution does.

Our solution uses IPE coordinates to reduce beam search space and minimize beam training overhead. IPE coordinates are also used to select the optimal RVs/DVSs based on the current network topology.

In the absence of obstructions, the IEEE 802.11ad beam pair mechanism has demonstrated high overhead and latency due to the combination of handshaking and exhaustive scanning methods.

While, in the absence of obstructions, the proposed solution reduced system overhead and latency by exploiting OLI/IPE based on classic protocol. Moreover, we introduce a robust and fast location-aided beam alignment framework to exhibit resilience concerning this problem. Location-aided beam alignment formulated the optimum beam alignment as the solution based on OLI/IPE coordinates.

During the ATI access period, IEEE 802.11ad uses a single protocol to implement channel access. Thus, if the link is blocked or the RSS measurements fall below a predefined threshold, the SV repeats the handshake mechanism until the RSS measurements meet the transmission requirements.

In contrast, the proposed solution uses three protocols during the ATI access period: classic, cooperative, and extension protocols that contribute to addressing most of the expected limitations scenarios based on mmWave V2X.

In IEEE 802.11ad, the communication range is limited to obstructions, distance, transmission power, etc. As a result, vehicles out of range are unable to communicate with the SV.

Meanwhile, our solution incorporated an extension protocol to overcome the limited coverage area associated with using the mmWave channel based on the extension protocol.

In IEEE 802.11ad, if the established link is blocked by a dynamic obstacle and RSS drops below a predefined threshold. In this manner, for link re-establishment, IEEE 802.11ad repeats the beam sweeping through exhaustive searching until the RSS satisfies the conditions for transmission, which is a high source of delays.

In contrast, our solution eliminates dynamic link blockage and link re-establishment problems (beam misalignment) by selecting diverse RVs/DVSs within the group. As a result, if one of the relay vehicles is blocked, the other relay vehicles can provide a connection to the IV.

In IEEE 802.11ad, link establishment, re-transmissions, link blockage, and beam misalignment introduce random latency, which is exacerbated as the number of vehicles in the network increases.

In contrast, several promising approaches are included in the proposed solutions to minimize system overhead and latency, including IPE, NTLs, MHC-REQ and ECR-REQ, and diverse RVs/DVSs.

VI. RESULTS

A. SIMULATION SCENARIOS

We performed exhaustive numerical simulations to compare the proposed solution with conventional mmWave V2V communications in the out-of-coverage environment. MATLAB, ray tracing, and additional simulation tools have been used to evaluate the performance of the proposed solution and path loss model. Furthermore, different types of propagation paths have been considered. Performance was measured using simulations at the 60GHz band and 2.16GHz channel.

We investigate the effects of obstructing vehicles on V2X networks with different vehicle types and densities in a mobile environment. Simulations are being conducted to investigate the impact of obstructions on mmWave V2V communications and verify the proposed model. Each vehicle is equipped with a proposed protocol, with a 50ms data exchange interval between the transmitter and receiver, which supports the use of periodic cooperative awareness beacons [10].

The SV transmits the DP within the intended communication range of a 300 m circle radius. In this approach, the effect of link obstruction was analyzed for each time instant, whereas the position of the SV serves as a reference for identifying vehicles in the intended communication range, as well as the IV in LOS, and NLOS scenarios. Furthermore, the position and status (static/dynamic) of all vehicles in the communication range were recorded at each time instant, regardless of whether they were in the LOS or NLOS. The simulations were performed on an urban scenario of 2 km long with four-lane and traffic intersections. To simulate realistic vehicular densities in Jamsil County, Seoul, a road surveillance camera (RSC) was used to record the approximate number of vehicles in the case of low, medium, and high-density scenarios.

Based on map layouts derived from OpenStreetMap, realistic environments comparable to those found in the Jamsil area were generated in the simulation, such as buildings, lakes, trees, vehicles, etc. Then the simulation of urban mobility (SUMO) [76] was used to perform the traffic simulation of the simulated topology with specific vehicle types, length, height, and width. SUMO is capable of automatically building simulation topologies and simulating vehicle motions. After obtaining the actual road topology of Jamsil County from OpenStreetMap, the mobility traces were converted to SUMO and then imported into Wireless inSite for evaluating the model performance. The final performance was evaluated using MATLAB simulations by comparing IEEE 802.11ad against the proposal. The simulation evaluated several parameters that significantly affected performance, including the probability of outages, SINR, data rate, throughput, adaptive channel estimation time, and packet delivery ratio. Additionally, to assess the performance of the proposed protocol, the RSRP threshold value was set at -115 dBm in the simulation.

B. CHANNEL CHARACTERISTICS

Knowledge of the channel characteristics is crucial for designing mmWave V2X communication channels. Accordingly, blockages, path losses, and large-scale/small-scale fading characteristics are substantial factors for accurately representing channel conditions and determining the link budget [9], [77].

However, in this study, the propagation characteristics were designed separately for LOS and NLOS scenarios owing to the propagation characteristics of the vehicular network topology, which are highly dependent on the LOS and NLOS links. Moreover, the RSRP at the RX-based IV was used to evaluate the link's performance based on the LOS and NLOS links. We investigated the proposed methodology on urban roads where blockage, path loss, and small/large fading effects strongly influence the mmWave V2X channel performance. Naka gaming-based path loss and fading models were used to classify the statistics of signals over a multipath fading channel and under different fading conditions according to the probability distribution [78].

C. NUMERICAL RESULTS

In Fig. 6 (a), we evaluated the outage probabilities of the proposed and conventional protocols as a function of densities. Generally, an outage occurs when the signal switches from LOS to NLOS, and the RSS level drops below a predefined threshold. Therefore, distinguishing between LOS/NLOS propagation is critical to computing outage probability.

As observed in Fig. 6 (a), the outage probability is directly proportional to traffic density. That is because a high number of vehicles causes more obstruction. Therefore, obstructing LOS and NLOS vehicles leads to significant attenuation and packet loss, resulting in increased outage probability.

However, the proposed protocol guarantees that the probability of the RSS is higher than a predefined threshold. As a result, compared to the traditional solution, the proposed solution maintains continuous connectivity throughout all scenarios, including harsh ones.

According to [46], the SINR value is influential in determining signal quality and is strongly affected by distance and blockages. In this paper, we analyzed the distribution of instantaneous SINR based on blockage probability and considered the path loss model as a function of traffic density. In Fig. 6 (b), the simulation results show the cumulative distribution function (CDF) as a function of SINR in the three density scenarios low, medium, and high. However, IEEE 802.11ad at 60 GHZ showed the lowest SINR in the case of blockage. It was observed that the SINR values of the conventional IEEE 802.11ad deteriorated significantly owing to harsh obstacles, which led to the worst propagation loss. The SINR values increased gradually as traffic density decreased, and vice versa. As a result, a significant disparity was observed in the SINR values of conventional IEEE 802.11ad for medium and high density. Meanwhile, the

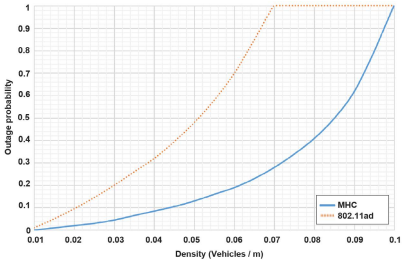

(a) Outage Probability as a Function of Vehicles Density at 60 GHz.

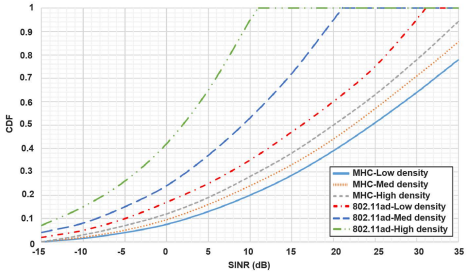

(b) Cumulative Density Function (CDF) of SINR vs varying Vehicles Density at 60 GHz

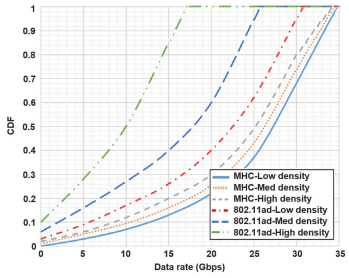

(c) Cumulative Density Function (CDF) of Transmitted Data Rate vs Varying Vehicles Density in,f= 60 GHz

FIGURE 6. Simulation results.

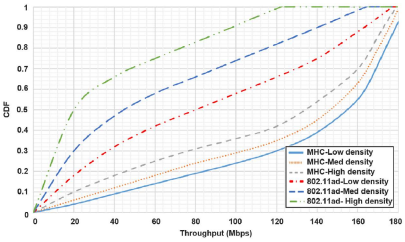

(a) Cumulative Density Function (CDF) of Throughput vs Varying Vehicles Density in, f= 60 GHz.

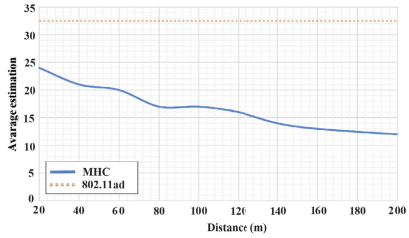

(b) Distance vs LOS-based average channel estimation time.

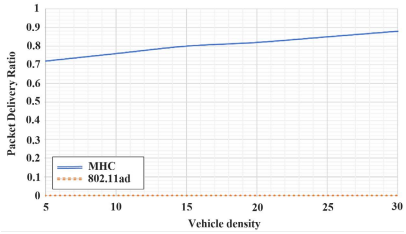

(c) Packet delivery ratio-based extension protocol vs density.

FIGURE 7. Simulation results.

proposed solutions exhibited a relatively small variation in the SINR value in most comparison scenarios. This is due to the truth that most of the received RSS values for the proposed protocol have exceeded a predefined threshold despite the difference in traffic density.

Interestingly, the proposed scheme is superior to the conventional approach regardless of traffic density, distance, and vehicle sizes. This superiority occurred because RVs sought to improve the link rather than block it by acting as an intermediary between SV and IV during transmission time.

As exemplified, IEEE 802.11ad SINR performance is about (15-50) dB lower than the proposed solution. The SINR of the conventional protocol drops rapidly when obstacles block the link. This is because signal fading may occur due to fading variations caused by blocked LOS and variations in the TX and RX antenna positions. However, random variations in the location of the TX and RX antennas lead to random variations in the received power. As a result, the SINR is strongly affected by frequent changes in vehicle location resulting in the state changing from LOS to NLOS.

Simulation results demonstrate that even with the strict limitations of the mmWave propagation, the SINR performance of the proposed solution is near comparable to that of the ideal solution.

The average achievable data rate in mmWave systems is heavily influenced by LOS and NLOS, which in turn are affected by vehicle densities, sizes, and distance.

Fig. 6 (c) shows the CDF of the proposal and IEEE 802.11ad as a function of data rates and densities. Typically, when vehicle density increases, blockage probabilities increase, and data rates decrease, which is consistent with common sense. The simulation shows that under all scenarios of different densities, the proposed protocol exhibits a slight decrease in data rate performance compared to the conventional protocol.

According to Fig. 6 (c), the proposed protocol can boost data rates by 50.9.

Since the proposed MHC minimizes the distance between transmitter and receiver by exploiting NVs such as RVs. As a result, high power is likely to be received with lower path losses than IEEE 802.11ad.

The CDF-based throughput for both IEEE 802.11ad and the proposed MHC is described in Fig. 7 (a). We show the impact of different vehicle densities on the throughput of both schemes.

The difference in throughput is mainly a result of the impact of obstacles, which leads to low channel quality. The mmWave link achieves almost zero throughputs, or they get outages in a heavy-density environment even at a close distance [28].

Observations indicate that throughput performance significantly improved with the proposed scheme. This is mainly because the proposed solution reduces the effects of the obstacles. It is worth mentioning that IEEE 802.11ad has a lower

throughput performance in the case of high traffic density, about 80% of the vehicles are in an outage, and only around 20% can achieve an acceptable rate.

Consequently, if the number of vehicles increases, the probability of a blockage increases dramatically, and network throughput decreases. Therefore, the throughput of the IEEE 802.11ad is acceptable in the case of low traffic density. It is noticeable that even when the LOS and NLOS links of the transmitter are blocked, the proposed system exhibits higher performance and less deterioration. Observations have shown that, in most traffic environments, the proposed protocols perform better than the conventional protocol by up to (75.

In order to evaluate the performance of the proposed classic protocol based on the beam acquisition, Fig. 7 (b) demonstrates a comparison between the proposed protocol and the IEEE 802.11ad from the perspective of the average channel estimation time against the distance. However, in the simulation, a communication range is assumed to be 200 meters, and the propagation model is performed under the LOS link without obstacles between nodes for accurate results. As expected, when the channel location is unknown, the channel estimation takes the longest time and is unaffected by distance. As reported in Fig. 7 (b), in IEEE 802.11ad-based LOS and EBS, the average channel estimation is approximately constant with distance. This is due to the fact that exhaustive beam searches blindly examine all possible beam pairs to determine the best beam pairs. In contrast, the proposed solution-based LOS and IPE showed a gradual decrease in channel estimation time as separation increased. This is because, with increasing separation distance, AOD/AOA range becomes narrower, resulting in narrow-sounding channels.

Finally, Fig. 7 (c) illustrates the effective measurement of the packet delivery ratio (PDR) in light of varying vehicle densities for the proposed extension protocol against IEEE 802.11ad. As demonstrated in the simulation, traffic density significantly impacts the performance of the overall protocol. According to Fig. 7 (c), the proportion of packets delivered by the proposed protocol increases as vehicle density increases. This is because, as vehicle density increases, the number of NVs within the communication range increases. Thus, more NVs candidates can be obtained as DVS, and at the same time, more NVs candidates can be selected as RVs by DVS if a cooperative protocol is adopted for the final DPD. While under all density scenarios, the IEEE 802.11ad achieved zero PDR measurements. This is because the IV is beyond the coverage area of the SV. Thus, the SV is not capable of communicating and sending a DP to the IV.

VII. CONCLUSION

We proposed a novel solution based on classic, cooperative, and extension protocols for mmWave V2X with or without a cellular network, which can achieve better performance than conventional approaches. Moreover, we provide an outlook of proposed enhancements for IEEE 802.11ad and its adaptability to IEEE 802.11bd or other mmWave V2X technologies. Extensive simulation results demonstrate that channel conditions are adequate to guarantee contentment, signal quality, and sufficient signal spread even when considering an extremely harsh environment. Overall, the perspective of the proposed design objective is to provide potential solutions to several technical challenges that significantly affect the operation of V2X-based mmWave frequencies in terms of improved beam alignment, achieving accurate beam acquisition, mitigating the effect of link obstruction, mitigating the impact of misalignment, increased the effective coverage range, and minimized end-to-end latency. Therefore, our approach can be a radical solution and achieve robust and reliable V2X-based mmWave vehicular communications. In future work, the proposed solution will be compared with the case of a random choice of the next relay to simplify the algorithm, e. g relay selection based on the Poisson field of nodes.

REFERENCES

[1] A. Bensrhair and T. Bapin, "Autonomous vehicle: What legal issues," in From AI to Autonomous and Connected Vehicles: Advanced Driver-Assistance Systems (ADAS), Aug. 2021.

[2] G. Naik, B. Choudhury, and J.-M. Park, "IEEE 802.11bd 5G NR V2X: Evolution of radio access technologies for V2X communications," *IEEE Access*, vol. 7, pp. 70169–70184, 2019.

[3] J. B. Kenney, "Dedicated short-range communications (DSRC) standards in the United States," *Proc. IEEE*, vol. 99, no. 7, pp. 1162–1182, Dec. 2011.

[4] R. Molina-Masegosa and J. Gozalvez, "LTE-V for sidelink 5G V2X vehicular communications: A new 5G technology for short-range vehicle-to-everything communications," *IEEE Veh. Technol. Mag.*, vol. 12, no. 4, pp. 30–39, Dec. 2017.

[5] J. Choi, V. Va, N. G.-Prelcic, R. Daniels, C. R. Bhat, and R. W. Heath, "Millimeter-wave vehicular communication to support massive automotive sensing," *IEEE Commun. Mag.*, vol. 54, no. 12, pp. 160–167, Dec. 2016.

[6] C. Wang, T. Shimizu, H. Muralidharan, and A. Yamamuro, "Demo: A real-time high-definition vehicular sensor data sharing system using millimeter wave V2 V communications," in *Proc. IEEE Veh. Net. Conf. (VNC)*, Dec. 2020, pp. 1–2.

[7] M. Giordani, M. Mezzavilla, and M. Zorzi, "Initial access in 5G mmWave cellular networks," *IEEE Commun. Mag.*, vol. 54, no. 11, pp. 40–47, Nov. 2016.

[8] F. Jameel, S. Wyne, S. J. Nawaz, and Z. Chang, "Propagation channels for mmWave vehicular communications: State-of-the-art and future research directions," *IEEE Wireless Commun.*, vol. 26, no. 1, pp. 144–150, Feb. 2019.

[9] V. Ratnam, H. Chen, S. Pawar, B. Zhang, C. Zhang, Y. Kim, S. Lee, and M. Cho, "FadeNet: Deep learning-based mm-wave large-scale channel fading prediction and its applications," *IEEE Access*, vol. 9, pp. 2169–3536, 2020.

[10] B. Schulz, "802.11ad—WLAN at 60 GHz: A technology introduction," Rohde & Schwarz, Munich, Germany, White Paper 1MA220_3e, Nov. 2017. Accessed: Sep. 5, 2018. [Online]. Available: https://cdn.rohdeschwarz.com/pws/dl_downloads/dl_application/application_notes/1ma220/1MA220_ 3e_WLAN_11ad_WP.pdf

[11] *802.11 NGV Proposed PAR*, Standard 802.11-18/0861r8, Study Group on 802.11bd (TGbd), IEEE, May 2019.

[12] B. Sadeghi, *802.11bd Functional Requirements Document*, Standard IEEE 802.11-19/0495r2, Manhattan, NY, USA, Mar. 2019.

[13] *Study on NR Vehicular to Everything (V2X) (Release 16)*, Standard v16.0.0, 3GPP TR 38.885, Mar. 2019.

[14] T. Zugno, M. Drago, M. Giordani, M. Polese, and M. Zorzi, "NR V2X communications at millimeter waves: An End-to-end performance evaluation," in *Proc. GLOBECOM IEEE Global Commun. Conf.*, Dec. 2020, pp. 2–6.

[15] S. Chen, J. Hu, Y. Shi, L. Zhao, and W. Li, "A vision of C-V2X: Technologies, field testing, and challenges with Chinese development," *IEEE Internet Things J.*, vol. 7, no. 5, pp. 3872–3881, May 2020.

[16] *Draft Standard for Information Technology-Telecommunications and Information Exchange Between Systems-Local and Metropolitan Area Networks-Specific Requirements—Part 11: Wireless LAN Medium Access Control (MAC) and Physical Layer (PHY) Specifications-Amendment 4: Enhancements for Very High Throughput in the 60 Ghz Band*, Standard P802.11ad/D9.0, Oct. 2012.

[17] *IEEE 802.11ad-Amendment 3: Enhancements for Very High Throughput in the 60 GHz Band*, Standard 802.11 Working Group, Dec. 2012.

[18] *Enhancements for Very High Throughput in the 60 GHz Band*, Standard 802.11ad 3, Mar. 2014.

[19] T.-W. Chang, L.-H. Shen, and K.-T. Feng, "Learning-based beam training algorithms for IEEE802.11ad/ay networks," in *Proc. IEEE 89th Veh. Technol. Conf. (VTC-Spring)*, Apr. 2019, pp. 1–4.

[20] L.-H. Shen, K.-T. Feng, and L. Hanzo, "Coordinated multiple access point multiuser beamforming training protocol for millimeter wave WLANs," *IEEE Trans. Veh. Technol.*, vol. 69, no. 11, pp. 13875–13889, Nov. 2020.

[21] B. Coll-Perales, M. Gruteser, and J. Gozalvez, "Evaluation of IEEE 802.11ad for mmWave V2V communications," in *Proc. IEEE Wireless Commun. Netw. Conf. Workshops (WCNCW)*, Apr. 2018, pp. 290–295.

[22] A. N. Uwaechia and N. M. Mahyuddin, "A comprehensive survey on millimeter wave communications for fifth-generation wireless networks: Feasibility and challenges," *IEEE Access*, vol. 8, pp. 62367–62414, 2020.

[23] G. Han, S. Kim, and J. Choi, "Multi-vehicle velocity estimation using IEEE 802.11ad waveform," in *Proc. IEEE Int. Conf. Acoust., Speech Signal Process. (ICASSP)*, Jun. 2021, pp. 4550–4553.

[24] T. Zugno, M. Drago, M. Giordani, M. Polese, and M. Zorzi, "Toward standardization of millimeter-wave vehicle-to-vehicle networks: Open challenges and performance evaluation," *IEEE Commun. Mag.*, vol. 58, no. 9, pp. 79–85, Sep. 2020.

[25] M. Giordani, A. Zanella, and M. Zorzi, "Millimeter wave communication in vehicular networks: Challenges and opportunities," in *Proc. 6th Int. Conf. Modern Circuits Syst. Technol. (MOCAST)*, May 2017, pp. 1–3.

[26] Z. Li, T. Yu, R. Fukatsu, G. K. Tran, and K. Sakaguchi, "Towards safe automated driving: Design of software-defined dynamic mmWave V2X networks and PoC implementation," *IEEE Open J. Veh. Technol.*, vol. 2, pp. 78–93, 2021.

[27] T. Shimizu, V. Va, G. Bansal, and R. W. Heath, "Millimeter wave V2X communications: Use cases and design considerations of beam management," in *Proc. Asia–Pacific Microw. Conf. (APMC)*, Nov. 2018, pp. 183–185.

[28] M. U. Sheikh, J. Hamalainen, G. D. Gonzalez, R. Jantti, and O. Gonsa, "Usability benefits and challenges in mmWave V2 V communications: A case study," in *Proc. Int. Conf. Wireless Mobile Comput., Netw. Commun. (WiMob)*, Oct. 2019, pp. 1–5.

[29] C. K. Anjinappa and I. Guvenc, "Millimeter-wave V2X channels: Propagation statistics, beamforming, and blockage," in *Proc. IEEE 88th Veh. Technol. Conf. (VTC-Fall)*, Aug. 2018, pp. 1–5.

[30] B. Chang, X. Yan, L. Zhang, Z. Chen, L. Li, and M. A. Imran, "Joint communication and control for mmWave/THz beam alignment in V2X networks," *IEEE Internet Things J.*, vol. 9, no. 13, pp. 11203–11213, Jul. 2022.

[31] V. Petrov, J. Kokkoniemi, D. Moltchanov, J. Lehtomäki, M. Juntti, and Y. Koucheryavy, "The impact of interference from the side lanes on mmWave/THz band V2V communication systems with directional antennas," *IEEE Trans. Veh. Technol.*, vol. 67, no. 6, pp. 5028–5041, Jan. 2018.

[32] C. Han and Y. Chen, "Propagation modeling for wireless communications in the terahertz band," *IEEE Commun. Mag.*, vol. 56, no. 6, pp. 96–101, Jun. 2018.

[33] T. S. Rappaport, S. Sun, R. Mayzus, H. Zhao, Y. Azar, K. Wang, G. N. Wong, J. K. Schulz, M. Samimi, and F. Gutierrez, "Millimeter wave mobile communications for 5G cellular: It will work!" *IEEE Access*, vol. 1, pp. 335–349, 2013.

[34] N. Garcia, H. Wymeersch, E. G. Ström, and D. Slock, "Location-aided mm-wave channel estimation for vehicular communication," in *Proc. IEEE Workshop Signal Process. Adv. Wireless Commun.*, Jul. 2016, pp. 1–5.

[35] W. Junsheng, C. Yawen, L. Zhaoming, W. Xiangming, and W. Zifan, "A low-complexity beam searching method for fast handover in mmWave vehicular networks," in *Proc. IEEE Wireless Commun. Netw. Conf. Workshop (WCNCW)*, Apr. 2019, pp. 1–6.

[36] I. Orikumhi, J. Kang, and S. Kim, "Location-aided window based beam alignment for mmWave communications," in *Proc. 7th IEEE Int. Conf. Netw. Intell. Digit. Content (IC-NIDC)*, Nov. 2021, pp. 1–5.

[37] I. Mavromatis, A. Tassi, R. J. Piechocki, and A. Nix, "MmWave system for future ITS: A MAC-layer approach for V2X beam steering," in *Proc. IEEE VTC*, Sep. 2017, pp. 1–6.

[38] Z. Li, L. Xiang, X. Ge, G. Mao, and H.-C. Chao, "Latency and reliability of mmWave multi-hop V2 V communications under relay selections," *IEEE Trans. Veh. Technol.*, vol. 69, no. 9, pp. 9807–9821, Sep. 2020.

[39] J. Lv, X. He, and T. Luo, "Blockage avoidance based sensor data dissemination in multi-hop mmWave vehicular networks," *IEEE Trans. Veh. Technol.*, vol. 70, no. 9, pp. 8898–8911, Sep. 2021.

[40] O. Rehman and M. Ould-Khaoua, "A hybrid relay node selection scheme for message dissemination in VANETs," *Future Gener. Comput. Syst.*, vol. 93, pp. 1–17, Apr. 2019.

[41] A. Zanella, A. Bazzi, and B. Masini, "Relay selection analysis for an opportunistic two-hop multi-user system in a Poisson field of nodes," *IEEE Trans. Commun.*, vol. 16, no. 2, pp. 1281–1293, Dec. 2016.

[42] W. Liu and Q. Du, "Multi-hop propagation-based computation offloading scheme in vehicular communication environment," in *Proc. IEEE 4th Adv. Inf. Manage., Communicates, Electron. Autom. Control Conf. (IMCEC)*, Jun. 2021, pp. 1–4.

[43] B. Coll-Perales, J. Gozalvez, and M. Gruteser, "Sub-6GHz assisted MAC for millimeter wave vehicular communications," *IEEE Commun. Mag.*, vol. 57, no. 3, pp. 125–131, Mar. 2019.

[44] S. Ket and R. N. Awale, "Receiver based capacity enhancement with cross-layer design approach for IEEE 802.11 ad-hoc networks," in *Proc. Int. Conf. Workshop Emerg. Trends Technol. (ICWET)*, Feb. 2011, pp. 804–809.

[45] M. Dahhani, A.-L. Beylot, and G. Jakllari, "On assessing the performance of IEEE 802.11ad beamforming training," *IEEE Trans. Netw. Service Manage.*, vol. 18, no. 3, pp. 3498–3508, Sep. 2021.

[46] W. Wu, Q. Shen, M. Wang, and X. Shen, "Performance analysis of IEEE 802.11.ad downlink hybrid beamforming," in *Proc. IEEE Int. Conf. Commun. (ICC)*, May 2017, pp. 2–4.

[47] M. Moradi, K. Thilakarathna, M. Ding, and M. Hassan, "Impact of device population on beam alignment performance of 802.11ad," in *Proc. IEEE Globecom. Conf. (GC Wkshps)*, Dec. 2018, pp. 1–5.

[48] R. W. Heath, N. González-Prelcic, S. Rangan, W. Roh, and A. M. Sayeed, "An overview of signal processing techniques for millimeter wave MIMO systems," *IEEE J. Sel. Topics Signal Process.*, vol. 10, no. 3, pp. 436–453, Apr. 2016.

[49] A. Patra, L. Simic, and M. Petrova, "Experimental evaluation of a novel fast beamsteering algorithm for link re-establishment in mm-wave indoor WLANs," in *Proc. IEEE 27th Annu. Int. Symp. Pers., Indoor, Mobile Radio Commun. (PIMRC)*, Sep. 2016, pp. 1–4.

[50] L. Niu and D. Liu, "Performance evaluation of unslotted CSMA/CA algorithm in wireless sensor networks," in *Proc. IEEE 5th Inf. Technol. Mechatronics Eng. Conf. (ITOEC)*, Jun. 2020, pp. 1–3.

[51] A. Bazzi, B. M. Masini, A. Zanella, and I. Thibault, "On the performance of IEEE 802.11p and LTE-V2V for the cooperative awareness of connected vehicles," *IEEE Trans. Veh. Technol.*, vol. 66, no. 11, pp. 10419–10432, Nov. 2017.

[52] *SI TC ITS, Intelligent Transport Systems; Vehicular Communications; Basic Set of Applications; Facilities Layer Protocols and Communication Requirements for Infrastructure Services*, Standard 103 301 V.1.1.1, 2016.

[53] G. S. Dahman and R. H. M. Hafez, "Angle-of-departure-aided opportunistic space-division multiple access," in *Proc. 7th Annu. Commun. Netw. Services Res. Conf.*, May 2009, pp. 2–7.

[54] O. El Ayach, S. Rajagopal, S. Abu-Surra, Z. Pi, and R. W. Heath, Jr., "Spatially sparse precoding in millimeter wave MIMO systems," *IEEE Trans. Wireless Commun.*, vol. 13, no. 3, pp. 1499–1513, Jan. 2014.

[55] A. Alkhateeb, O. El Ayach, G. Leus, and R. W. Heath, Jr., "Channel estimation and hybrid precoding for millimeter wave cellular systems," *IEEE J. Sel. Topics Signal Process.*, vol. 8, no. 5, pp. 831–846, Oct. 2014.

[56] A. Abdallah, A. Celik, M. M. Mansour, and A. M. Eltawil, "Deep learning-based frequency-selective channel estimation for hybrid mmWave MIMO systems," *IEEE Trans. Wireless Commun.*, vol. 21, no. 6, pp. 3804–3821, Jun. 2022.

[57] S. Campbell, N. O'Mahony, L. Krpalcova, D. Riordan, J. Walsh, A. Murphy, and C. Ryan, "Sensor technology in autonomous vehicles: A review," in *Proc. IEEE 29th Irish. Conf. Irish Sign. Syst. (ISSC)*, Jun. 2018, pp. 1–5.

[58] B. Pardhasaradhi, P. Srihari, and P. Aparna, "Navigation in GPS spoofed environment using M-best positioning algorithm and data association," *IEEE Access*, vol. 9, pp. 51536–51549, 2021.
[59] L. Heng, T. Walter, P. Enge, and G. X. Gao, "GNSS multipath and jamming mitigation using high-mask-angle antennas and multiple constellations," *IEEE Trans. Intell. Transp. Syst.*, vol. 16, no. 2, pp. 741–750, Apr. 2015.
[60] F. Hui and F. Qin, "Influence of inertial sensor errors on GNSS/INS integrated navigation performance," in *Proc. 8th Int. Conf. Measuring Technol. Mechatronics Autom. (ICMTMA)*, Mar. 2016, pp. 1–5.
[61] S. Marano, W. M. Gifford, H. Wymeersch, and M. Z. Win, "NLOS identification and mitigation for localization," *IEEE J. Sel. Areas Commun.*, vol. 28, no. 7, pp. 1026–1035, Sep. 2010.
[62] J. Mullane, B.-N. Vo, M. D. Adams, and B.-T. Vo, "A random-finite-set approach to Bayesian SLAM," *IEEE Trans. Robot.*, vol. 27, no. 2, pp. 268–282, Apr. 2011.
[63] G. Bresson, Z. Alsayed, L. Yu, and S. Glaser, "Simultaneous localization and mapping: A survey of current trends in autonomous driving," *IEEE Trans. Intell. Veh.*, vol. 2, no. 3, pp. 194–220, Sep. 2017.
[64] R. Liu, J. Wang, and B. Zhang, "High definition map for automated driving: Overview and analysis," *J. Navigat.*, vol. 73, no. 2, pp. 324–341, Mar. 2020.
[65] R.-T. Juang, "MAP aided self-positioning based on LIDAR perception for autonomous vehicles," in *Proc. 4th Asia–Pacific Conf. Intell. Robot Syst. (ACIRS)*, Jul. 2019, pp. 1–5.
[66] C. Guo, M. Lin, H. Guo, P. Liang, and E. Cheng, "Coarse-to-fine semantic localization with HD map for autonomous driving in structural scenes," in *Proc. IEEE/RSJ Int. Conf. Intell. Robots Syst. (IROS)*, Sep. 2021, pp. 1–5.
[67] M. Herb, M. Lemberger, M. M. Schmitt, A. Kurz, T. Weiherer, N. Navab, and F. Tombari, "Semantic image alignment for vehicle localization," in *Proc. IEEE/RSJ Int. Conf. Intell. Robots Syst. (IROS)*, Sep. 2021, pp. 1–4.
[68] M. Ulmschneider and C. Gentner, "RANSAC for exchanging maps in multipath assisted positioning," in *Proc. IEEE Int. Conf. Ind. Cyber Phys. Syst. (ICPS)*, May 2019, pp. 1–4.
[69] F. de Ponte Müller, E. M. Diaz, B. Kloiber, and T. Strang, "Bayesian cooperative relative vehicle positioning using pseudorange differences," in *Proc. IEEE/ION Position, Location Navigat. Symp. (PLANS)*, May 2014, pp. 434–444.
[70] O. K. Tonguz, N. Wisitpongphan, and F. Bai, "DV-CAST: A distributed vehicular broadcast protocol for vehicular ad hoc networks," *IEEE Wireless Commun.*, vol. 17, no. 2, pp. 47–57, Apr. 2010.
[71] J. Lee, M. Kang, J. Oh, and Y. H. Lee, "Space-time alignment for channel estimation in millimeter wave communication with beam sweeping," in *Proc. GLOBECOM IEEE Global Commun. Conf.*, Dec. 2017, pp. 2–7.
[72] S. Rezaie, C. N. Manchon, and E. de Carvalho, "Location- and orientation-aided millimeter wave beam selection using deep learning," in *Proc. IEEE Int. Conf. Commun. (ICC)*, Jun. 2020, pp. 1–6.
[73] W. Santipach and M. L. Honig, "Optimization of training and feedback overhead for beamforming over block fading channels," *IEEE Trans. Inf. Theory*, vol. 56, no. 12, pp. 6103–6115, Dec. 2010.
[74] *Study on Downlink Multiuser Superposition Transmission for LTE*, Standard 3GPP, RP250456, 3rd Generation Partnership Project, Mar. 2015.
[75] M. A. Hoque and M. S. Khan, "An experimental investigation of multi-hop V2 V communication delays using WSMP," in *Proc. SoutheastCon*, Apr. 2019, pp. 2–5.
[76] M. A. D. Khumara, L. Fauziyyah, and P. Kristalina, "Estimation of urban traffic state using simulation of urban mobility(SUMO) to optimize intelligent transport system in smart city," in *Proc. Int. Electron. Symp. Eng. Technol. Appl. (IES-ETA)*, Oct. 2018, pp. 2–7.
[77] S. Sun, G. R. MacCartney, M. K. Samimi, and T. S. Rappaport, "Synthesizing omnidirectional received power and path loss from directional measurements at millimeter-wave frequencies," in *Proc. IEEE Global. Conf. Commun. (GLOBECOM), Dec. 2015*, pp. 2–6.
[78] L. Cheng, B. E. Henty, D. D. Stancil, F. Bai, and P. Mudalige, "Mobile vehicle-to-vehicle narrow-band channel measurement and characterization of the 5.9 GHz dedicated short range communication (DSRC) frequency band," *IEEE J. Sel. Areas Commun.*, vol. 25, no. 8, pp. 1501–1516, Oct. 2007.

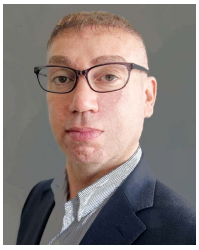

RAFID I. ABD (Member, IEEE) received the B.S. degree in electronics and communications engineering from the University of Technology, in 2004, the M.S. degree in communications and network from the University of Portsmout, in 2009, and the M.S. degree in electronics and communications from the University of SKKU, in 2015. He is currently pursuing the Ph.D. degree with the School of Electrical and Electronic Engineering, Yonsei University, Seoul, South Korea. Since 2016, he has been involved in research and invention in the communications and information transmission industry. His research interests include wireless communication and signal processing, including mmWave communications and vehicular communication. He received several awards and patents related to wireless communication technology.

KWANG SOON KIM (Senior Member, IEEE) received the B.S. *(summa cum laude)*, M.S.E., and Ph.D. degrees in electrical engineering from the Korea Advanced Institute of Science and Technology (KAIST), Daejeon, South Korea, in February 1994, February 1996, and February 1999, respectively. From March 1999 to March 2000, he was a Postdoctoral Researcher at the Department of Electrical and Computer Engineering, University of California at San Diego, La Jolla, CA, USA. From April 2000 to February 2004, he was a Senior Member of Research Staff at the Mobile Telecommunication Research Laboratory, Electronics and Telecommunication Research Institute, Daejeon. Since March 2004, he has been with the Department of Electrical and Electronic Engineering, Yonsei University, Seoul, South Korea, where he is currently a Professor. His research interests include signal processing, communication theory, information theory, and stochastic geometry applied to wireless heterogeneous cellular networks, wireless local area networks, wireless D2D networks, wireless ad hoc networks, and new radio access technologies for 5G. He was a recipient of the Postdoctoral Fellowship from the Korea Science and Engineering Foundation (KOSEF), in 1999. He received the Outstanding Researcher Award from the Electronics and Telecommunication Research Institute (ETRI), in 2002, the Jack Neubauer Memorial Award (Best System Paper Award, IEEE TRANSACTIONS ON VEHICULAR TECHNOLOGY) from IEEE Vehicular Technology Society, in 2008, and the LG Research and Development Award: Industry-Academic Cooperation Prize, LG Electronics, in 2013. From 2006 to 2012, he was the Editor of the *Journal of the Korean Institute of Communications and Information Sciences* (KICS). From 2009 to 2014, he was the Editor of the IEEE TRANSACTIONS ON WIRELESS COMMUNICATIONS. From 2013 to 2016, he was the Editor-in-Chief of the *Journal of KICS*. Since 2008, he has been the Editor of the *Journal of Communications and Networks* (JCN).